Bioorganic Chemistry 88 (2019) 102918

Contents lists available at ScienceDirect

Bioorganic Chemistry

journal homepage: www.elsevier.com/locate/bioorg

Potent and selective EGFR inhibitors based on 5-aryl-7*H*-pyrrolopyrimidin-4-amines

Ann Christin Reiersølmoen[a], Thomas Ihle Aarhus[a,b], Sarah Eckelt[a,c], Kristin Gabestad Nørsett[d,e], Eirik Sundby[b], Bård Helge Hoff[a,*]

[a] Department of Chemistry, Norwegian University of Science and Technology (NTNU), NO-7491 Trondheim, Norway
[b] Department of Material Science, Norwegian University of Science and Technology (NTNU), NO-7491 Trondheim, Norway
[c] Institute of Organic Chemistry, Universität Hamburg, Welckerstrasse 8, 201354 Hamburg, Germany
[d] Department of Biomedical Laboratory Science, Norwegian University of Science and Technology (NTNU), NO-7491 Trondheim, Norway
[e] Department of Computer Science, Norwegian University of Science and Technology (NTNU), NO-7491 Trondheim, Norway

ARTICLE INFO

Keywords:
Pyrrolopyrimidine
EGFR
Erlotinib
Kinase
Chiral drug
(*S*)-phenylglycinol

ABSTRACT

The epidermal growth factor receptor represents an important target in cancer therapy, and low molecular weight inhibitors based on quinazolines have reached the marked. Herein we report on a new scaffold, 5-aryl-7*H*-pyrrolo[2,3-*d*]pyrimidin-4-amines, and show that when employing (*S*)-phenylglycinol as C-4 substituent, potent inhibitors can be made. The two most active inhibitors have suitable druglike properties, were equipotent with Erlotinib in Ba/F3 cell studies, and showed lower cross reactivity than Erlotinib in a panel of 50 kinases.

1. Introduction

The epidermal growth factor receptor (EGFR/HER1) is often amplified, overexpressed or mutated in solid tumours, and is therefore a potential target in cancerous diseases [1–4]. Most importantly, in non-small-cell lung cancer the activating EGFR mutations L858R and exon 19 deletions account for approximately 90% of the primary EGFR dysregulation [1,3]. For patients harbouring these mutations, EGFR inhibitor therapy increases progression free survival [5,6]. Moreover, this tyrosine kinase receptor also appears attractive in management of pain [7]. Excessive EGFR signalling can be regulated by monoclonal antibodies targeting the extracellular part of the receptor complex or small molecular inhibitors with intracellular activity. Approved ATP competitive EGFR inhibitors include quinazolines with anilines at C-4 such as Erlotinib, Gefitinib, Lapatinib (Fig. 1) and Vandetanib [8,9], while irreversible EGFR inhibitors such as Afatinib and Dacomitinib are also based on the same scaffold. Our research has instead focused on pyrrolo- [10,11], furo- [12] and thieno[2,3-*d*]pyrimidines [13,14] based structures containing chiral benzylamines instead of anilines at C-4 (structures I-III, Fig. 1).

During investigation of possible kinase related mechanisms for IL-17 secretion inhibitors [15], we discovered that one 5-aryl-7*H*-pyrrolo[2,3-*d*]pyrimidin-4-amine, compound **IV** in Fig. 1, was a potent EGFR inhibitor. Thus, our aim was to identify new selective EGFR inhibitors based on the 5-arylpyrrolopyrimidine scaffold.

2. Result and discussion

2.1. Synthesis

Our previous compound collection of 5-arylated pyrrolopyrimidines [15], was extended with structures containing variations at position 4, different 5-aryl groups, and three different substituents at the N-7 of the pyrrole. Firstly, 5-arylated-7*H*-pyrrolo[2,3-*d*]pyrimidin-4-amines containing (*R*)-1-phenylethylamine and (*S*)-phenylglycinol at C-4 were prepared since these substitution patterns have been valuable in the development of 6-arylated-7*H*-pyrrolo[2,3-*d*]pyrimidin-4-amine based EGFR inhibitors [10,11]. The route utilised is shown in Scheme 1. In short, 4-chloro-pyrrolo[2,3-*d*]pyrimidine (**1**) was iodinated cleanly at C-5 giving compound **2** in 81–85% yield. 4-Chloro-5-iodo-7*H*-pyrrolo [2,3-*d*]pyrimidine (**2**) proved unstable under thermal amination reactions, thus the pyrrole nitrogen was protected with 2-(trimethylsilyl) ethoxymethyl (SEM), allowing for facile amination to the advanced intermediates **4** and **5**. The following Suzuki cross-coupling performed

* Corresponding author at: Department of Chemistry, Norwegian University of Science and Technology, Høgskoleringen 5, NO-7491 Trondheim, Norway.
E-mail addresses: Ann.C.Reiersolmoen@ntnu.no (A.C. Reiersølmoen), Thomas.Aarhus@ntnu.no (T.I. Aarhus), Kristin.Norsett@ntnu.no (K.G. Nørsett), Eirik.Sundby@ntnu.no (E. Sundby), bard.helge.hoff@chem.ntnu.no (B.H. Hoff).

https://doi.org/10.1016/j.bioorg.2019.102918
Received 2 January 2019; Received in revised form 1 March 2019; Accepted 8 April 2019
Available online 11 April 2019

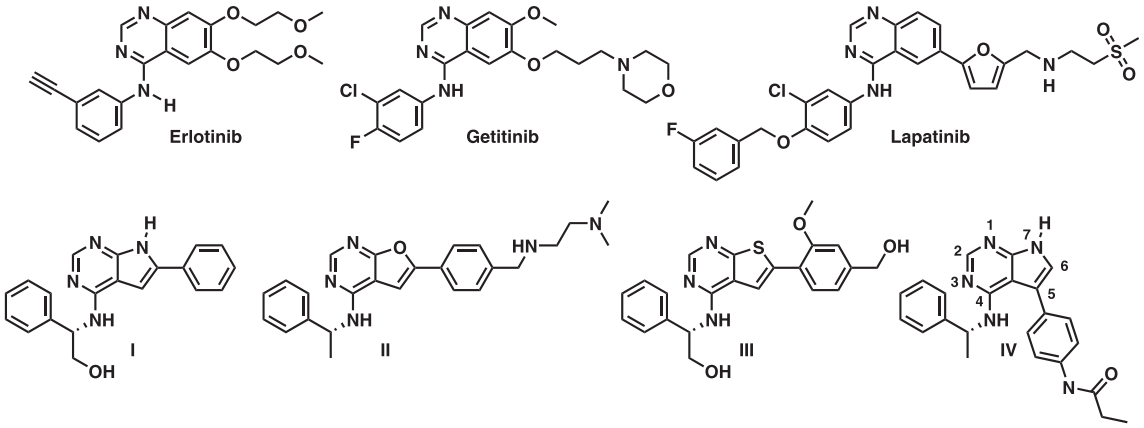

Fig. 1. Structure of the approved EGFR inhibitors Erlotinib, Gefitinib and Lapatinib and the investigational EGFR inhibitors **I-IV**. The numbering system of 5-arylated-7*H*-pyrrolo[2,3-*d*]pyrimidin-4-amines is also shown.

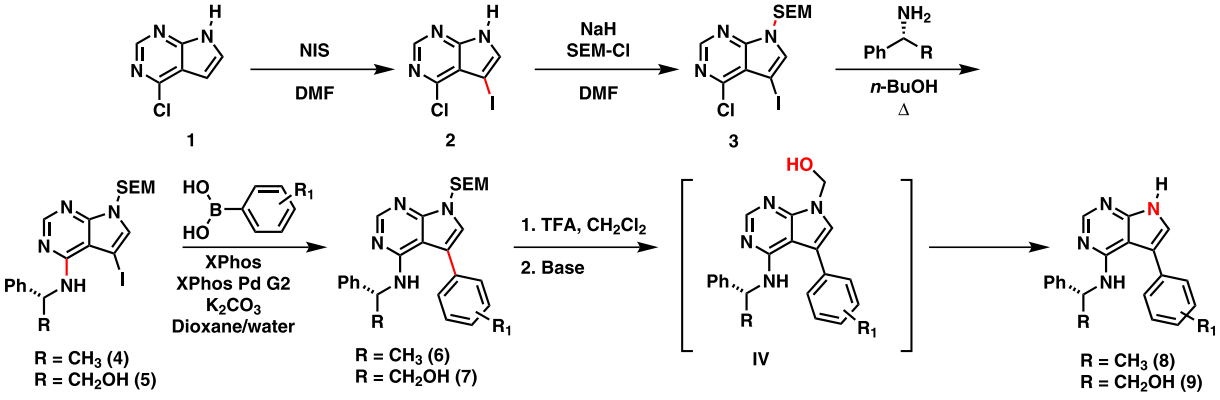

Scheme 1. Synthesis of pyrrolopyrimidines **8** and **9**.

with 5 mol% of XPhos and XPhos second generation pre-catalyst gave the structures **6** and **7** in non-optimized yields of 47–96%. The reaction time varied from 5 min to 3 h.

Removal of the SEM-group was done by a two-step procedure. Firstly, compound **6** or **7** was treated with trifluoroacetic acid until ^{1}H NMR analysis indicated full consumption of starting material. At this stage, the reaction mixture contained a blend of intermediate **IV** and the product. Then, further reaction with bases such as sodium bicarbonate, ammonia or sodium hydroxide converted the intermediate **IV** to **8** or **9**. None of the reaction proceeded with ease, and several additions of base were required. In cases when conversion had halted, an extractive work-up followed by evaporation, and restarting the reaction was found efficient. Possibly, there is an equilibrium between the intermediate **IV**, the target product and formaldehyde, which is displaced by removal of formaldehyde in the evaporation.

We also aimed to investigate if this scaffold was suitable for developing irreversible inhibitors towards the EGFR^{T790M} mutant. To install an acrylic moiety at the 5-aryl group the route shown in Scheme 2 was utilised. The *para*-nitro derivative **6f** was reduced using iron powder giving 83% yield of the aniline **6j**. Acylation with acryloyl chloride resulted in derivative **6k** (94% yield). The following SEM-deprotection proved more difficult. Upon heating at 50 °C with trifluoroacetic acid (TFA), the main component isolated was the debenzylated analogue **10k** (32% yield). However, when the TFA treatment was done at 22 °C, the target product **8k** was obtained, though in a low 25% yield. Apparently, an acid catalysed debenzylation occurs more readily on this derivative than the others. A similar debenzylation was utilised on quinazolines by Becherer et al. [16].

Several binding poses are possible for small molecules within the active site of EGFR. To explore these opportunities, previously made materials and new derivatives substituted at *N*-7 with methoxybenzyl, **13b**, and *N,N*-dimethylethylamine, **15l**, were included in the study. Synthesis of the latter two derivatives are shown in Scheme 2.

2.2. EGFR kinase inhibition

The prepared compounds were first assayed for their EGFR enzymatic inhibitory properties at 100 nM test concentration, see Fig. 2. The phenyl substituted parent compound **8a** showed 73% inhibition. Encouragingly, all the 5-aryl substituted derivatives in this series showed an increase in potency (89–93% inhibition, Fig. 2). Compound **8k** containing an electrophilic acrylamide moiety was intended as an irreversible inhibitor for targeting cysteines. Unfortunately, assay towards the EGFR^{T790M} mutant showed that **8k** had a neglectable activity towards this kinase (data not shown).

In line with that previously seen for the corresponding 6-arylpyrrolopyrimidines [10,11], higher activity was noticed when the amino group was changed to (*S*)-phenylglycinol (compounds **9a-b**, **9e** and **9i**). Also in this series, substitution of the 5-aryl group increased potency as compared to the parent compound **9a**.

For compounds with other substitution patterns, the acrylate **10k**, was completely inactive towards native EGFR and showed only 20% inhibition of EGFR^{T790M} at 500 nM test concentration. Further, the *N*-7 *para*-methoxybenzyl substituted **13b**, and all compound in which the pyrrole function was masked as *N,N*-dimethylaminoethyl (comp. **15b**, **15l**, **17b**, **19b**, **19i**, **19l** and **19p**) were inactive. In contrast, when the

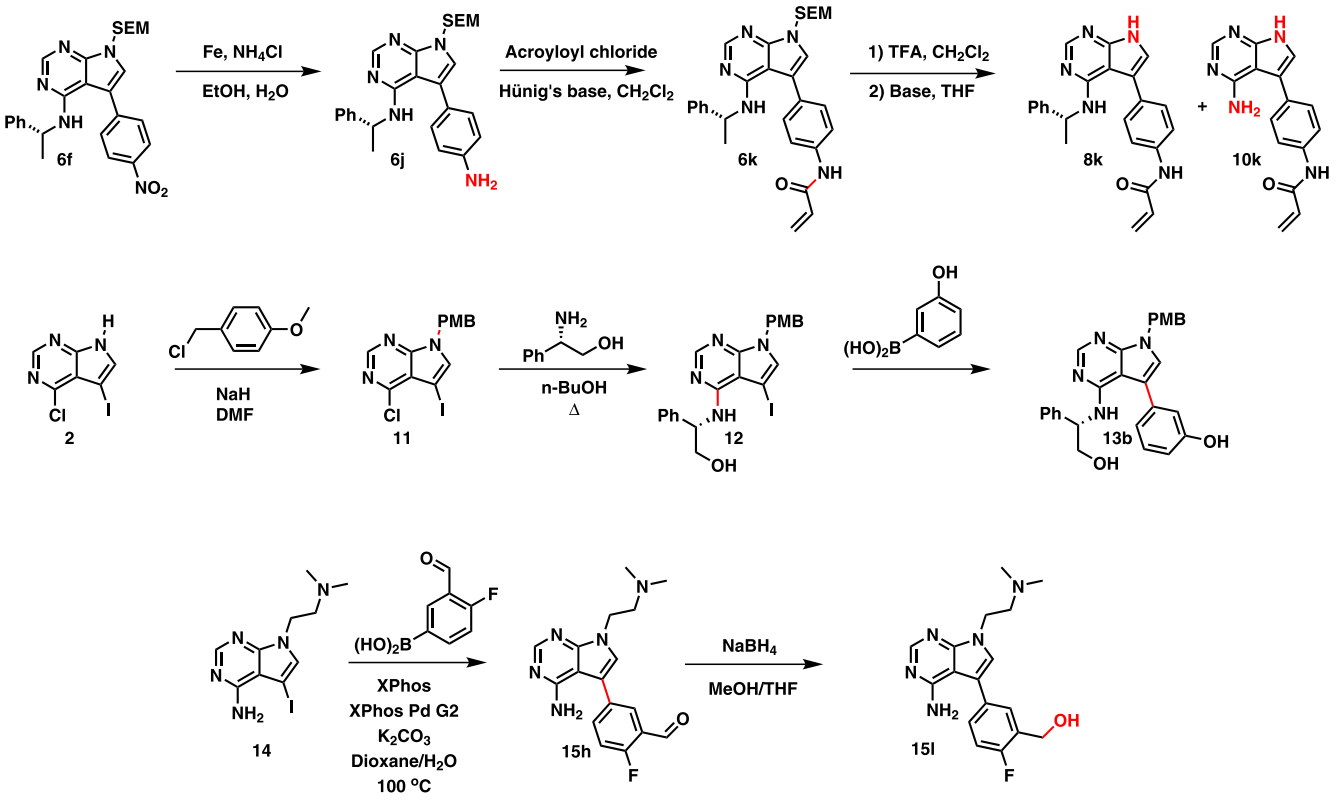

Scheme 2. Synthetic routes to the acrylate derivatives **8k** and **10k** and the pyrrole substituted derivatives **13b** and **15l**.

pyrrole function was methylated as in compound **16b**, or when containing the rather bulky aniline at C-4, decent 76% and 58% inhibition were observed. This shows that the pyrrole function is not crucial for activity and that further engineering of the 4-amino group might be possible to improve the properties or activity of the compounds.

Some of the more potent antagonists were further assayed for their IC_{50}-values. The results are summarised in Table 1 alongside calculated metrics for drug-like properties including ligand efficiency (LE) [17], binding efficiency (BEI) [18], surface efficiency index (SEI) [18], and ligand-efficiency-dependent lipophilicity (LELP) [19]. Equations for calculating these metrics can be found in the Supplementary data file. LE and BEI values, which quantifies activity per heavy atom or molecular mass, should be as high as possible. SEI-values (target 5–25 [18]) describes how dependent activity is of polarity, with low values indicating that activity is highly dependent of polar groups. Finally, LELP describes how dependent the activity is of lipophilic groups by dividing calculated logP by LE. LELP values below 10 is preferable.

In the (*R*)-1-phenylethylamine series of compounds, the IC_{50} values were in the range of 2–16 nM (entries 1–5). The most potent derivative was the propionamide **8n** (entry 4). However, due to its higher molecular weight, the computed druglike properties rather suggest that further development should be based on compounds with lower molecular weight like **8b** or **8 m** (entries 1 and 3).

The (*S*)-phenylglycinol substituted derivatives **9** (entries 6–9) possessed higher activity. The most potent analogue was the 3-hydroxy derivative **9b** with an IC_{50} of 0.9 nM. The commercial drug Erlotinib had an IC_{50} of 0.5 nM (entry 11). However, due to lower molecular weight and more balanced polarity, the druglike metrics of this latter series of derivatives compares favourably with that of Erlotinib. The IC_{50} curves of Erlotinib, **9b** and **9e** are shown in Fig. 3. As a reference, the methylated derivative **16b** (entry 10) was also included in the assay, with an IC_{50} of 62 nM.

2.3. In silico evaluation of binding mode

Docking using GLIDE in extra precision (XP) mode using Schrödinger Maestro [20–22], and molecular dynamics using the Desmond suite, the OPL3 force field and the TIP4P solvent model [23] were employed to investigate binding poses of the most potent derivatives **9a**, **9b**, **9e**, and **9i**. The X-ray structure used was 2J6M (3.1 Å) of the EGFR kinase domain in complex with AEE788 [24]. Docking suggested two possible binding modes to the hinge region within the ATP binding pocket. These are visualised as the 10 ns dynamics interaction plots in Fig. 4 for compound **9b**. The docking scores are given in the Supplementary data file (Table S2).

In binding pose I (Fig. 4, left), preferred by compounds **9a** and **9e**, the inhibitors have two hydrogen bonding interactions to Met793. The α-NH group of Met793 donates a hydrogen bond to the pyrimidine N-1, and the oxygen of the carbonyl group accepts a hydrogen bond from the pyrrole-NH. Further, pyrimidine N-3 is engaged in a water mediated hydrogen bond to Thr854. The (*S*)-phenylglycinol unit is located in a lipophilic pocket with size limitations, and the aromatic part is indicated to have cation-π interaction with Lys745. The 5-aryl group is pointing outwards towards the solvent exposed area. This binding mode is similar to that seen for Erlotinib [25,26] and Gefitinib [24].

In the alternative binding pose II, indicated by docking to be preferred by inhibitor **9b** and **9i**, the antagonists have one hydrogen bond to Met793, while the pyrrole-NH donates a hydrogen bond to Gln791. This type of hydrogen bonding has also been postulated for an 2-(*ortho*-hydroxyphenyl)-4-aminoquinazoline [27] and a pyrrolopyrimidine based inhibitor [28]. In contrast to binding pose I, the (*S*)-phenylglycinol unit is directed towards the solvent exposed area, while the 5-aryl group is located into the lipophilic small pocket. Dynamics in case **9b** suggests that binding is promoted by hydrogen bonding from the 3-hydroxyl directly to Asp855 and via a water molecule to Arg841. Additionally, a cation-π interaction is postulated with Lys745. According to dynamics, binding pose II is preferred for **9b** and **9i** due to stronger hydrogen bonding interactions involving the aromatic hydroxyl group.

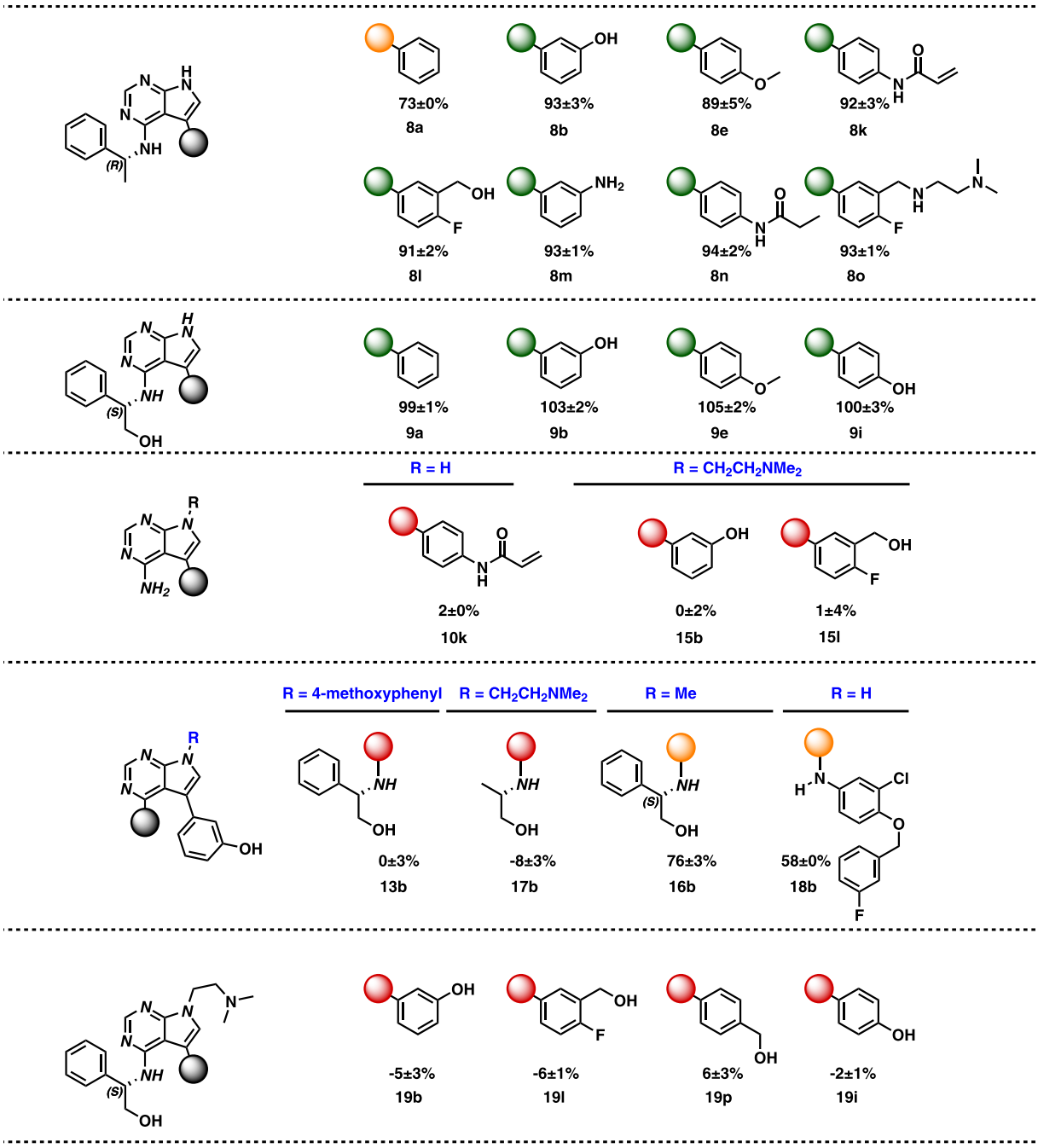

Fig. 2. Inhibition (%) of EGFR at 100 nM test concentration.

The superimposed docked structures of **9b** in binding mode I and II are shown in Fig. 5. Interestingly, both the lipophilic parts and the two hydroxyl groups in the two poses overlay fairly well. For comparison the docked structure of **9a** is overlaid by the docked structure of the corresponding 6-phenyl derivative (compound **I**, Fig. 1) [11], previously found to be a cell potent EGFR inhibitor. However, more conclusive evidence of binding mode cannot be obtained without X-ray co-crystal structures.

2.4. Kinase selectivity and cell potency

Even though Erlotinib is regarded as a rather selective kinase inhibitor, it has some side effects [29,30]. To identify potential off-targets and reveal selectivity differences, the most potent derivatives were assays for their inhibition towards 50 additional kinases at 500 nM test concentration. The different profiles plotted as % remaining activity are shown in Fig. 6.

These curves can be used to evaluate selectivity scores [31]. Using 50% inhibition at 500 nM as the threshold for the calculation, selectivity scores followed the order **9b**: 0.04 > **9e**: 0.06 > **9i**: 0.08 > Erlotinib: 0.1. Thus, the 5-arylated pyrrolopyrimidines might have an advantage over Erlotinib in terms of kinase selectivity and thus off-target related toxicity.

Fig. 7 compares the 10 most potent off-targets for Erlotinib, **9b**, **9e** and **9i** (16 kinases altogether), ranked by activity towards Erlotinib. The commercial drug Erlotinib, showed stronger inhibition towards ERBB4, ABL1, KDR, LYN A and B, RET, FLT4, Aurora B and SRC than the new inhibitors. Rather similar potency was observed towards ERBB2, LCK and FGR, MAPK8 and YES, while the **9**-series were clearly more potent towards protein kinase C alpha (PRKCA) and glycogen

Table 1
EGFR IC_{50} values and druglike properties of 5-aryl-7*H*-pyrrolo[2,3-*d*]pyrimidin-4-amines.

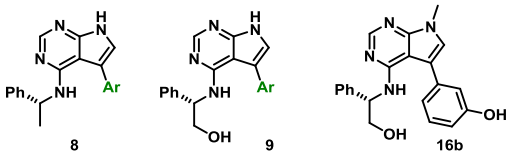

Entry	Comp.	Ar	EGFR IC_{50} (nM)	LE	BEI	SEI	LELP
1	**8b**		9 ± 1[a]	0.32	24.4	10.9	10.7
2	**8l**	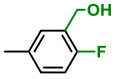	16 ± 1 [a]	0.29	21.5	10.6	11.4
3	**8m**	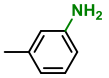	13 ± 1[a]	0.32	23.9	9.9	9.8
4	**8n**	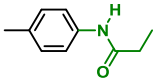	2.1 ± 0.8 [a]	0.29	22.2	10.3	13.4
5	**8o**	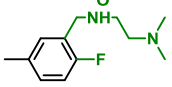	11 ± 2 [a]	0.25	18.4	11.6	11.8
6	**9a**		3.1 ± 0.4 [b]	0.34	25.8	11.5	8.4
7	**9b**		0.9 ± 0.0 [b]	0.35	26.1	9.6	7.2
8	**9e**	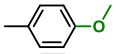	1.2 ± 0.2 [b]	0.33	24.8	10.7	8.4
9	**9i**	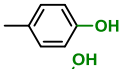	1.6 ± 0.3 [b]	0.34	25.4	9.4	7.4
10	**16b**		62 ± 24 [a]	0.27	20.0	8.7	9.9
11	Erlotinib[c]		0.5 ± 0.0 [b]	0.32	23.6	12.4	9.6

[a] Mean value of two titration curves (20 data points) and standard deviation.
[b] Mean value of four titration curves (40 data points) and standard deviation.
[c] For structure see Fig. 1.

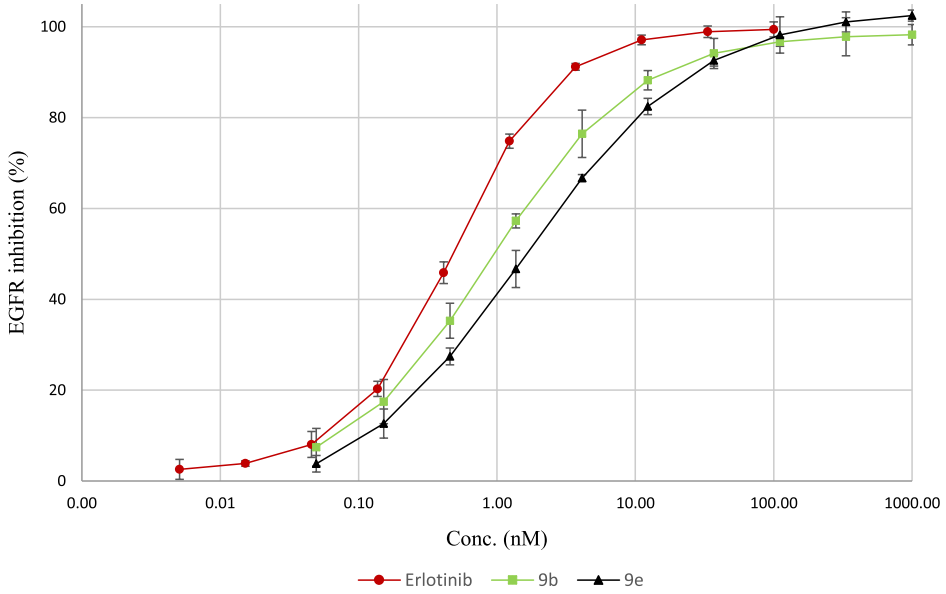

Fig. 3. EGFR IC_{50} measurements compound **9b** (IC_{50}: 0.9 nM), **9e** (IC_{50}: 1.2 nM) and Erlotinib (IC_{50}: 0.5 nM) based on 40 data points each.

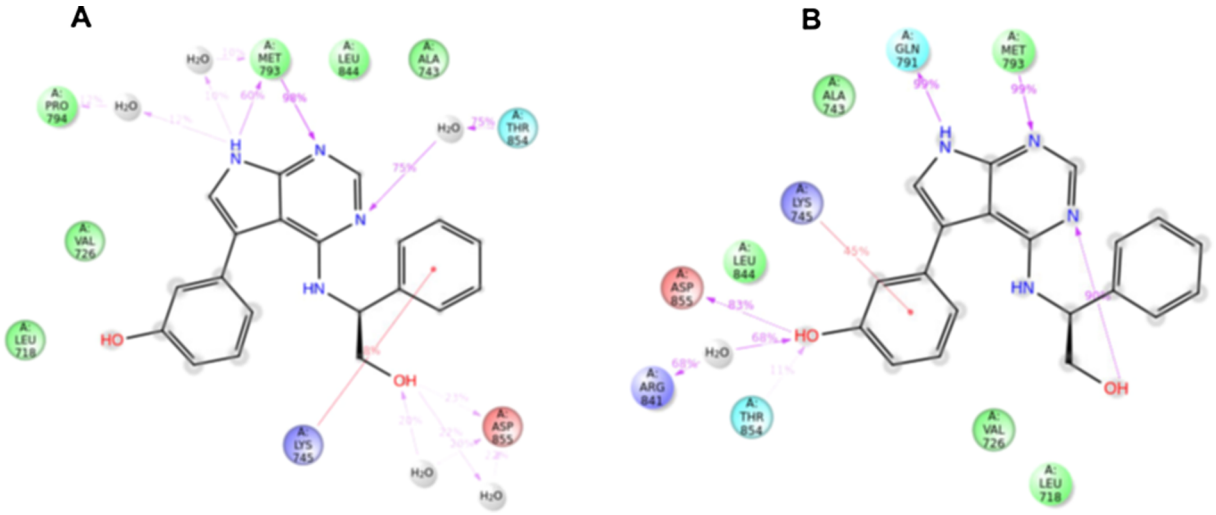

Fig. 4. Dynamic interaction map after 10 ns simulations. A: Binding pose I, preferred by inhibitors **9a** and **9e** involving two hydrogen bonds between the inhibitors and Met793. B: Binding pose II preferred by inhibitors **9b** and **9i** in which the core part of the structure binds to Met793 and Gln791.

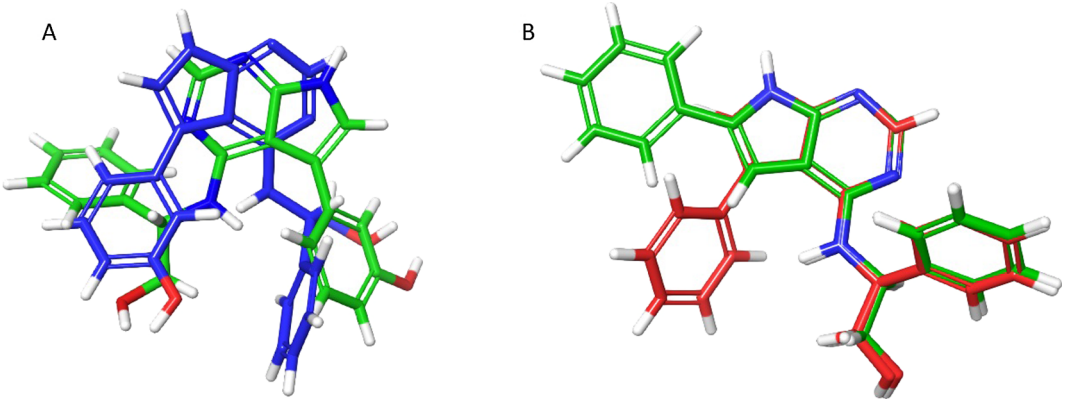

Fig. 5. A: Compound **9b** after docking with EGFR in binding mode I (green) and binding mode II (blue); B: Compound **9a** (red) after docking in binding mode I (red) overlaid by the docked structure of the corresponding 6-phenyl analogue (comp **I**) (green).

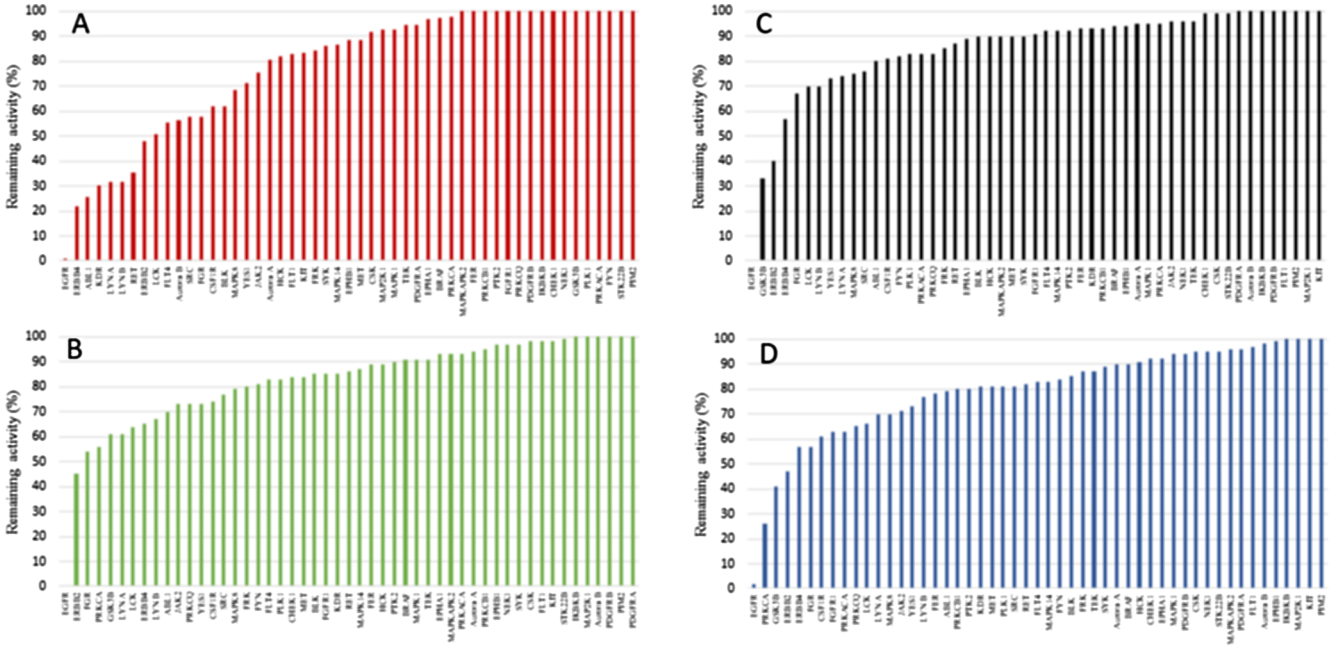

Fig. 6. Residual activity for different kinases after treatment with 500 nM test compound. A = Erlotinib, B: **9b**; C: **9e** and D: **9i**.

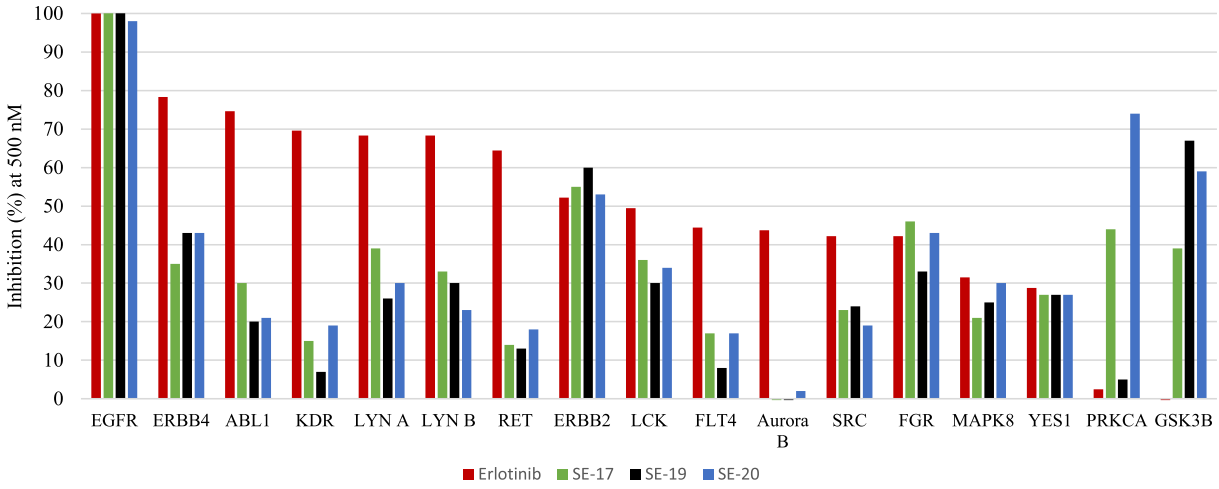

Fig. 7. Comparison of inhibition (%) of the ten most important off-targets for Erlotinib, **9b**, **9e** and **9i**.

synthase kinase 3 beta (GSK3B). Targeting PRKCA might be relevant in breast cancers [32,33], and *in vitro* studies have also indicated the involvement of PRKCA in Erlotinib resistance in lung cancer models [34]. GSK3B is found to plays a vital role in cellular processes among others in autophagy, and is regarded as a potential target in cancer research [35].

Point mutation L858R is one of the primary mutations in EGFR driven non-small cell lung cancer (NSCLC). The cellular potency of four of the 5-arylpyrrolopyrimidines were compared with Erlotinib using Ba/F3-EGFR^{L858R} reporter cells [36] with the XTT assay. In line with the enzymatic EGFR assay, the 3-hydroxy and 4-methoxy derivatives **9b** (IC_{50}: 112 nM) and **9e** (IC_{50}: 104 nM) showed potent inhibition of cell viability in line with that of Erlotinib (IC_{50}: 95 nM), see Fig. 8. The unsubstituted derivative **9a** and the 4-hydroxy derivative **9i** were also highly active with IC_{50} of 221 nM and 272 nM, respectively. Thus, 5-arylpyrrolopyrimidines appears as an attractive scaffold for obtaining cell active EGFR inhibitors.

3. Conclusion

5-Aryl-7*H*-pyrrolopyrimidin-4-amines has previously not been investigated as EGFR inhibitors. Herein we describe their synthesis and enzymatic inhibition towards EGFR. By employing (*S*)-phenylglycinol as C-4 substituent, potent derivatives with suitable calculated druglike properties were obtained. Docking suggests that this compound class might have two possible binding modes, in which the 4-amino and 6-aryl group switch positions. Proliferation study using NSCLC model cells, Ba/F3-EGFR^{L858R}, revealed two of the derivatives to be equipotent to Erlotinib. Moreover, these two derivatives were more selective than Erlotinib as evidenced by assay in a panel of 50 kinases. Thus, 5-aryl-7*H*-pyrrolopyrimidin-4-amine appears as an excellent scaffold for developing EGFR inhibitors, and the two most potent derivatives identified could be highly valuable for EGFR mechanistically studies.

4. Experimental

4.1. General

K_2CO_3, XPhos, XPhos 2. generation pre-catalyst, $NaBH_4$, and arylboronic acid were obtained from Sigma-Aldrich. 4-Chloro-7*H*-pyrrolo[2,3-*d*]pyrimidine was made in-house [10]. Silica-gel column chromatography was performed using silica-gel 60A from Fluka, pore size 40–63 μm. Celite 545 from Fluka was also used. Previously prepared compounds includes **2**, **3**, **4**, **8l**, **8n**, **8o**, **14**, **15b-19b**, **19i**, **19l** and **19q** [15].

4.2. Analysis

^{1}H and ^{13}C NMR spectra were recorded with Bruker Avance 400 and 600 spectrometers. operating at 400 MHz and 100 MHz, respectively. ^{19}F NMR was performed on a Bruker Avance 500 operating at 564 MHz. For ^{1}H and ^{13}C NMR chemical shifts are in ppm rel. to DMSO-d_6, while for ^{19}F NMR the shift values are relative to hexafluorobenzene. Coupling constants are in hertz. HPLC (Agilent 1100-Series) with a

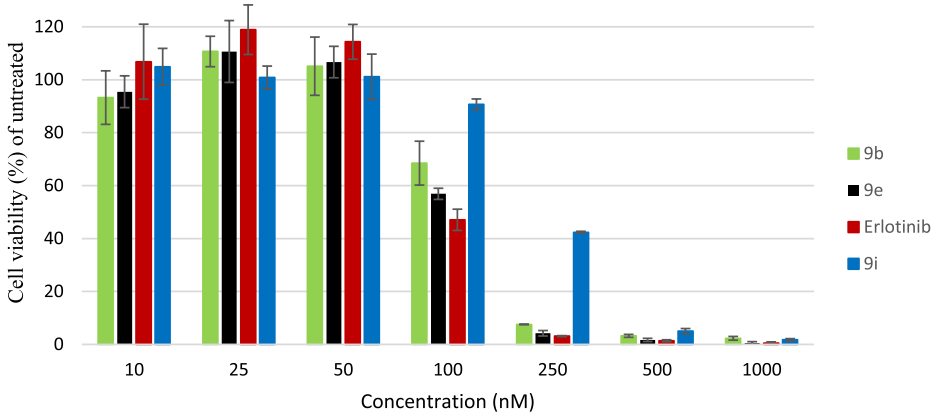

Fig. 8. Cell proliferation study of compounds **9b**, **9e** and **9i** compared to Erlotinib using Ba/F3-EGFR^{L858R} cells. Each data point shown is the average of three independent replicates. IC_{50}: Erlotinib: 95 ± 6 nM; **9b**: 112 ± 8 nM, **9e**: 104 ± 4 nM and **9i**: 221 ± 4 nM.

G1379A degasser, G1311A Quatpump, G1313A ALS autosampler and a G1315D Agilent detector (230 nm) was used to determine the purity of the synthesised compounds. Conditions: Poroshell C18 (100 × 4.6 mm) column, flow rate 0.8 mL/min, elution starting with water/CH_3CN (90/10), 5 min isocratic elution, then linear gradient elution for 35 min ending at CH_3CN/water (100/0). The software used with the HPLC was Agilent ChemStation. Accurate mass determination (ESI) was performed on an Agilent G1969 TOF MS instrument equipped with a dual electrospray ion source. Accurate mass determination in positive and negative mode was performed on a "Synapt G2-S" Q-TOF instrument from Waters. Samples were ionized by the use of an ASAP probe, no chromatography separation was used before the mass analysis. FTIR spectra were recorded on a Thermo Nicolet Avatar 330 infrared spectrophotometer. All melting points are uncorrected and measured by a Stuart automatic melting point SMP40 apparatus. Optical rotation was recorded using an Anton Paar Modular Circular Polarimeter 5100. Cells with a length of 10 mm or length of 2.5 mm were used to measure rotation at room temperature (22 °C).

4.3. Synthesis

4.3.1. General procedure for Suzuki-cross coupling

To a mixture of the selected arylboronic acid (0.610 mmol, 1.2 equiv.), K_2CO_3 (1.53 mmol, 3 equiv.), XPhos (0.0250 mmol, 0.05 equiv.), 2nd generation XPhos pre-catalyst (0.0250 mmol, 0.05 equiv.), and the selected 4-amino-5-iodo-7*H*-pyrrolo[2,3-*d*]pyrimidine (0.511 mmol, 1 equiv.) in 1,4-dioxane (3 mL) was added water (3 mL) under a nitrogen atmosphere. The reaction mixture was stirred at 100 °C until complete conversion. The solvent was removed before water (15 mL) and EtOAc (25 mL) were added, the phases were separated and the water phase was extracted with more EtOAc (3 × 20 mL). The combined organic phases were washed with brine (20 mL), dried over Na_2SO_4, filtered and concentrated. Purification was as stated for each individual compound.

4.3.2. (S)-2-((5-Iodo-7-((2-(trimethylsilyl)ethoxy)methyl)-7H-pyrrolo[2,3-d]pyrimidin-4-yl)amino)-2-phenylethan-1-ol (5)

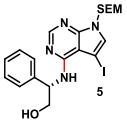

4-Chloro-5-iodo-7-(2-(trimetylsilyl)ethoxymethyl)-7*H*-pyrrolo[2,3-*d*]-pyrimidine (**3**) (1.01 g, 2.46 mmol) and (*S*)-phenylglycinol (0.837 g, 6.10 mmol) in *n*-butanol (8 mL) were stirred and heated at reflux for 6 h. The solvent was removed in vacuo before EtOAc (90 mL) and water (60 mL) were added. After phase separation the water phase was extracted with more EtOAc (3 × 70 mL) and the combined organic phases were dried over Na_2SO_4 and concentrated in vacuo. The product was purified by silica column chromatography (CH_2Cl_2/EtOAc, 5/1 + 3% Et_3N, R_f = 0.41) to give 1.11 g (2.18 mmol, 89%) of compound **5** which solidified to a colorless powder, mp. 88.5–90 °C; $[\alpha]_D^{20} = -28.0$ (c = 1.00, $CHCl_3$); ^{1}H NMR (400 MHz, DMSO-d_6): 8.12 (s, 1H), 7.61 (s, 1H), 7.39 (d, J = 7.6 Hz, 2H), 7.32 (t, J = 7.6 Hz, 2H), 7.25–7.21 (m, 1H), 7.07 (d, J = 7.6 Hz, 1H), 5.45 (s, 2H), 5.40–5.38 (m, 1H), 5.23 (t, J = 4.8 Hz, 1H), 3.88–3.71 (m, 2H), 3.50–3.46 (m, 2H), 0.82–0.78 (m, 2H), −0.09 (s, 9H); ^{13}C NMR (100 MHz, DMSO-d_6): 155.4, 152.1, 149.8, 141.4, 129.8, 128.2 (2C), 126.8, 126.6 (2C), 103.0, 72.1, 65.6, 64.7, 55.0, 51.0, 17.1, −1.40. IR (neat, cm^{-1}) ν: 3385 (m), 3120 (w), 1599 (s), 1245 (s), 1079 (s, br), 700 (s), 602 (m); HRMS (APCI/ASAP, m/z): found 511.1023 (calcd. $C_{20}H_{28}N_4O_2SiI$, 511.1026, $[M+H]^+$).

4.3.3. (R)-5-Phenyl-N-(1-phenylethyl)-7-((2-(trimethylsilyl)ethoxy)methyl)-7H-pyrrolo[2,3-d]pyrimidin-4-amine (6a)

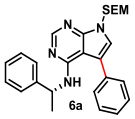

The synthesis was performed as described in Section 4.3.1, starting with compound **4** (227 mg, 0.511 mmol) and phenylboronic acid (109 mg, 0.610 mmol). The reaction time was 30 min. Purification by silica-gel column chromatography (*n*-pentane/EtOAc, 3/1, R_f = 0.50) gave 179 mg (0.403 mmol, 79%) of **6a** as an oil; $[\alpha]_D^{20} = -85.8$ (c 1.02, $CHCl_3$); ^{1}H NMR (400 MHz, DMSO-d_6): 8.23 (s, 1H), 7.51–7.49 (m, 4H), 7.46 (s, 1H), 7.42–7.40 (m, 1H), 7.32–7.26 (m, 4H), 7.23–7.20 (m, 1H), 5.54 (s, 2H), 5.39–5.32 (m, 1H), 5.52–5.50 (m, 1H), 3.56 (t, J = 8.1 Hz, 2H), 1.39 (d, J = 6.9 Hz, 3H), 0.84 (t, J = 8.1 Hz, 2H), −0.08 (s, 9H); ^{13}C NMR (100 MHz, DMSO-d_6): 155.3, 151.9, 150.4, 144.2, 134.4, 129.0 (2C), 128.6 (2C), 128.4 (2C), 127.2, 126.8, 125.8 (2C), 123.4, 115.8, 100.3, 72.3, 65.5, 49.5, 22.8, 17.2, −1.4 (3C); HRMS (APCI/ASAP+, m/z): found 445.2419 (calcd. $C_{26}H_{33}N_4OSi$, 445.2424 $[M+H]^+$).

4.3.4. (R)-3-(4-((1-Phenylethyl)amino)-7-((2-(trimethylsilyl)ethoxy)methyl)-7H-pyrrolo[2,3-d]pyrimidin-5-yl)phenol (6b)

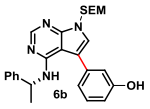

The synthesis was performed as described in Section 4.3.1, starting with compound **4** (150 mg, 0.303 mmol) and (3-hydroxyphenyl) boronic acid (49 mg, 0.356 mmol). The reaction time was 25 min. Purification by silica-gel column chromatography (*n*-pentane/EtOAc, 3/2, R_f = 0.54) gave **6b** as beige crystals, 131 mg (0.284 mmol, 94%), mp. 60–61C; $[\alpha]_D^{20} = -136.2$ (c 1.03, DMSO); ^{1}H NMR (600 MHz, DMSO-d_6): 9.71 (s, 1H), 8.21 (s, 1H), 7.41 (s, 1H), 7.30–7.27 (m, 5H), 7.22–7.20 (m, 1H), 6.91–6.90 (m, 1H), 6.90–6.89 (m, 1H), 6.82–6.80 (m, 1H), 5.67–5.65 (m, 1H), 5.53 (s, 2H), 5.36–5.31 (m, 1H), 3.55 (t, J = 8.1 Hz, 2H), 1.41 (d, J = 6.9 Hz, 3H), 0.83 (t, J = 8.1 Hz, 2H), −0.08 (s, 9H); ^{13}C NMR (150 MHz, DMSO-d_6): 157.9, 155.2, 151.9, 150.3, 144.3, 135.6, 130.2, 128.4 (2C), 126.8, 125.7 (2C), 123.1, 119.2, 115.9, 115.4, 114.3, 100.3, 72.2, 65.5, 49.5, 23.0, 17.1, −1.4 (3C); IR (neat, cm^{-1}): 3408 (w), 2947 (w, br), 1590 (m), 1570 (m), 1473 (m), 1286 (m), 1249 (m), 1172 (m), 1079 (m), 858 (m), 835 (s), 781 (m), 697 (s); HRMS (APCI/ASAP+, m/z): found 461.2366 (calcd. $C_{26}H_{33}N_4O_2Si$, 461.2373 $[M+H]^+$).

4.3.5. tert-Butyl-(R)-(3-(4-((1-phenylethyl)amino)-7-((2-(trimethylsilyl)ethoxy)methyl)-7H-pyrrolo[2,3-d]pyrimidin-5-yl)phenyl)carbamate (6c)

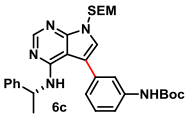

The synthesis was performed as described in Section 4.3.1, starting with compound **4** (498 mg, 1.22 mmol) and (3-((*tert*-butoxycarbonyl) amino)phenyl)boronic acid (930 mg, 6.73 mmol). The reaction time was 15 min. Purification by silica-gel column chromatography (*n*-pentane/EtOAc, 3/1, R_f = 0.33) gave **6c** as a white foam, 577 mg (1.03 mmol, 84%); $[\alpha]_D^{20} = -94.1$ (c 0.98, DMSO); ^{1}H NMR (400 MHz, DMSO-d_6): 9.56 (s, 1H), 8.22 (s, 1H), 7.87 (s, 1H), 7.41 (s, 1H), 7.36–7.34 (m, 2H), 7.31–7.24 (m, 4H), 7.21–7.18 (m, 1H), 7.08–7.06 (m, 1H), 5.69–5.67 (m, 1H), 5.55 (s, 2H), 5.35–5.28 (m, 1H), 3.55 (t,

J = 8.2 Hz, 2H), 1.47 (s, 9H), 1.41 (m, 3H), 0.84 (t, J = 8.1 Hz, 2H), −0.08 (s, 9H); ^{13}C NMR (100 MHz, DMSO-d_6): 155.2, 152.8, 151.9, 150.4, 144.3, 140.3, 134.9, 129.5, 128.3 (2C), 126.7, 125.8 (2C), 123.3, 122.3, 117.7, 116.9, 116.0, 100.2, 79.2, 72.2, 65.5, 49.7, 28.1 (3C), 22.8, 17.1, −1.4 (3C); IR (neat, cm^{-1}): 3413 (w), 2956 (w), 1714 (m), 1584 (m), 1236 (m), 1153 (s), 1070 (m), 831 (m), 691 (m); HRMS (APCI/ASAP+, m/z): found 560.3046 (calcd. $C_{31}H_{42}N_5O_3Si$, 560.3057 $[M+H]^+$).

4.3.6. (R)-5-(3-Nitrophenyl)-N-(1-phenylethyl)-7-((2-(trimethylsilyl) ethoxy)methyl)-7H-pyrrolo[2,3-d]pyrimidin-4-amine (**6d**)

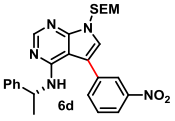

The synthesis was performed as described in Section 4.3.1, starting with compound **4** (998 mg, 2.44 mmol) and 3-nitrophenyboronic acid (930 mg, 6.73 mmol). The reaction time was 15 min. Purification by silica-gel column chromatography (*n*-pentane/EtOAc, 3/1, R_f = 0.27) gave the product **6d** as an yellow oil, 954 mg (1.95 mmol, 96%); $[\alpha]_D^{20}$ = −165.2 (c 1.01, DMSO); ^{1}H NMR (400 MHz, DMSO-d_6): 8.314–8.307 (m, 1H), 8.21 (s, 1H), 8.21–8.19 (m, 1H), 7.99–7.97 (m, 1H), 7.76–7.40 (m, 2H), 7.35–7.34 (m, 2H), 7.27–7.25 (m, 2H), 7.20–7.17 (m, 1H), 6.09–6.08 (m, 1H), 5.56 (s, 2H), 5.46–5.41 (m, 1H), 3.57 (t, J = 8.2 Hz, 2H), 1.44–1.43 (m, 3H), 0.84 (t, J = 8.1 Hz, 2H), −0.08 (s, 9H); ^{13}C NMR (100 MHz, DMSO-d_6): 155.3, 152.0, 151.1, 148.1, 144.6, 136.2, 134.5, 130.2 128.1 (2C), 126.5, 126.0 (2C), 125.0, 122.6, 121.3, 114.1, 99.8, 72.4, 65.6, 49.8, 22.5, 17.1, −1.4 (3C); IR (neat, cm^{-1}): 3438 (w), 2947 (w, br), 1587 (m), 1526 (m), 1466 (m), 1339 (s), 1242 (m), 1175 (m), 1075 (s), 831 (s), 691 (s); HRMS (APCI/ASAP+, m/z): found 490.2271 (calcd. $C_{26}H_{32}N_5O_3Si$, 490.2274 $[M+H]^+$).

4.3.7. (R)-5-(4-Methoxyphenyl)-N-(1-phenylethyl)-7-((2-(trimethylsilyl) ethoxy)methyl)-7H-pyrrolo[2,3-d]pyrimidin-4-amine (**6e**)

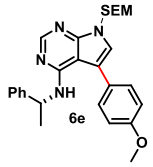

The synthesis was performed as described in Section 4.3.1, starting with compound **4** (349 mg, 0.853 mmol) and (4-methoxyphenyl) boronic acid (156 mg, 1.02 mmol). The reaction time was 5 min. Purification by silica-gel column chromatography (*n*-pentane/EtOAc, 3/1, R_f = 0.39) gave the product as a light brown oil, 323 mg (0.680 mmol, 79%); $[\alpha]_D^{20}$ = −106.1 (c 1.00, DMSO); ^{1}H NMR (600 MHz, DMSO-d_6): 8.21 (s, 1H), 7.42–7.41 (s, 2H), 7.36 (s, 1H), 7.31–7.26 (m, 4H), 7.23–7.21 (m, 1H), 7.06–7.05 (m, 2H), 5.53 (s, 2H), 5.48–5.47 (m, 1H), 5.36–5.31 (m, 1H), 3.81 (s, 3H), 3.55 (t, J = 8.2 Hz, 2H), 1.40 (d, J = 6.9 Hz, 3H), 0.83 (t, J = 8.1 Hz, 2H), −0.08 (s, 9H); ^{13}C NMR (150 MHz, DMSO-d_6): 158.6, 155.3, 151.8, 150.2, 144.2, 129.9 (2C),128.4 (2C), 126.9, 126.4, 125.8 (2C), 122.9, 115.4, 114.5 (2C), 100.5, 72.2, 65.5, 55.2, 49.5, 22.8, 17.1, −1.4 (3C); IR (neat, cm^{-1}): 3418 (w), 2951 (w, br), 1560 (s), 1470 (m), 1236 (s), 1086 (m), 831 (s), 691 (m); HRMS (APCI/ASAP+, m/z): found 475.2522 (calcd. $C_{27}H_{35}N_4O_2Si$, 475.2529 $[M+H]^+$).

4.3.8. (R)-5-(4-Nitrophenyl)-N-(1-phenylethyl)-7-((2-(trimethylsilyl) ethoxy)methyl)-7H-pyrrolo[2,3-d] pyrimidin-4-amine (**6f**)

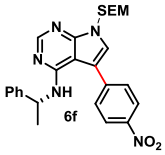

The synthesis was performed as described in Section 4.3.1, starting with compound **4** (350 mg, 0.710 mmol) and 4-nitrophenylboronic acid (144 mg, 0.870 mmol). The reaction time was 5 min. Purification by silica-gel column chromatography (*n*-pentane/EtOAc, 3/1, R_f = 0.33) gave 265 mg (0.541 mmol, 76%) of **6f** as a yellow gum; $[\alpha]_D^{20}$ = −126.9 (c 1.04, $CHCl_3$); ^{1}H NMR (400 MHz, DMSO-d_6): 8.31–8.29 (m, 2H), 8.25 (s, 1H), 7.77–7.75 (ap.d, 2H), 7.74 (s, 1H), 7.38–7.36 (ap.d, 2H), 7.31–7.27 (m, 2H), 7.23–7.19 (m, 1H), 6.08–6.06 (m, 1H), 5.56 (s, 2H), 5.46–5.39 (m, 1H), 3.56 (t, J = 8.1 Hz, 2H), 1.47 (d, J = 6.9 Hz, 3H), 0.84 (t, J = 8.1 Hz, 2H), −0.08 (s, 9H); ^{13}C NMR (100 MHz, DMSO-d_6):155.3, 152.1, 151.3, 154.8, 144.6, 141.7, 129.0 (2C), 128.2 (2C), 126.7, 126.1 (2C), 125.7, 124.1 (2C), 114.4, 99.7, 71.4, 65.7, 49.9, 22.5, 17.1, −1.4 (3C); IR (cm^{-1}, neat): 3432 (w), 2950 (w, br), 1734 (w),1560 (m), 1336 (s), 1246 (m), 1175 (m), 1075 (m), 831 (s), 751 (m), 701 (s); HRMS (APCI/ASAP+, m/z): found 490.2270 (calcd. $C_{26}H_{32}N_5O_3Si$, 490.2274 $[M+H]^+$).

4.3.9. tert-Butyl-(R)-(4-(4-((1-phenylethyl)amino)-7-((2-(trimethylsilyl) ethoxy)methyl)-7H-pyrrolo[2,3-d] pyrimidin-5-yl)phenyl)carbamate (**6g**)

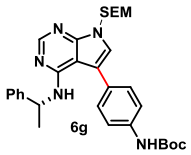

The synthesis was performed as described in Section 4.3.1, starting with compound **4** (350 mg, 0.710 mmol) and 4-(*N*-Boc-amino)phenylboronic acid (203 mg, 0.856 mmol). The reaction time was 10 min. Purification by silica-gel column chromatography (*n*-pentane/EtOAc, 3/1, R_f = 0.67) gave 352 mg (0.629 mmol, 89%) of **6 g** as a white solid; $[\alpha]_D^{20}$ = −124.7 (c 1.08, $CHCl_3$). ^{1}H NMR (400 MHz, DMSO-d_6): 9.49 (s, 1H), 8.20 (s, 1H), 7.59–7.57 (ap.d, 2H), 7.40–7.31 (ap.d, 2H), 7.37 (s, 1H), 5.76 (s, 2H), 7.31–7.26 (m, 4H), 7.23–7.19 (m, 1H), 5.57–5.56 (m, 1H), 5.39–5.32 (m, 1H), 3.54 (t, J = 8.1 Hz, 2H), 1.50 (s, 9H), 1.39 (d, J = 6.9 Hz, 3H), 0.83 (t, J = 8.1 Hz, 2H), −0.08 (s, 9H); ^{13}C NMR (100 MHz, DMSO-d_6): 155.3, 152.7, 151.8, 150.3, 144.3, 138.8, 128.9 (2C), 128.4 (2C), 127.8, 126.8, 125.7 (2C), 123.0, 118.5 (2C), 115.6, 100.4, 79.2, 72.2, 65.5, 49.5, 28.1 (3C), 23.0, 17.1, −1.4 (3C); HRMS (APCI/ASAP+, m/z): found 560.3057 (calcd. $C_{31}H_{42}N_5O_3Si$, 560.3057 $[M+H]^+$).

4.3.10. (R)-5-(4-Aminophenyl)-N-(1-phenylethyl)-7-((2-(trimethylsilyl) ethoxy)methyl)-7H-pyrrolo[2,3-d] pyrimidin-4-amine (**6j**)

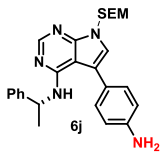

The nitro functionalised **6f** (250 mg, 0.511 mmol) was dissolved in EtOH (12 mL) and iron-powder (189 mg, 3.38 mmol), NH_4Cl (30.2 mg, 0.600 mmol) and water (3 mL) were added. The reaction mixture was stirred at 100 °C for 7 h, before an additional amount of NH_4Cl (15.0 mg, 0.269 mmol) was added. The reaction was stirred for an

additional hour to achieve full conversion. The mixture was filtered through a celite column. Then, water (30 mL) was added and the mixture was extracted with EtOAc (2 × 25 mL). The organic phases were washed with brine (25 mL), dried over Na_2SO_4 and concentrated in vacuo. Purification by silica-gel column chromatography (*n*-pentane/EtOAc, 1/1, $R_f = 0.38$) gave 194 mg (0.422 mmol, 83%) of **6j** as a yellow powder; $[\alpha]_D^{20} = -138.9$ (c 1.08, $CHCl_3$). ^{1}H NMR (400 MHz, DMSO-d_6): 8.17 (s, 1H), 7.32–7.20 (m, 5H), 7.23 (s, 1H), 7.16–7.14 (ap.d, 2H), 6.69–6.67 (ap.d, 2H), 5.75 (s, 2H), 5.57–5.56 (m, 1H), 5.39–5.32 (m, 1H), 5.26 (s, 2H), 3.53 (t, $J = 8.1$ Hz, 2H), 1.38 (d, $J = 6.9$ Hz, 3H), 0.84 (t, $J = 8.1$ Hz, 2H), −0.08 (s, 9H); ^{13}C NMR (100 MHz, DMSO-d_6): 155.4, 151.7, 150.0, 148.2, 144.3, 129.4 (2C), 128.4 (2C), 126.8, 125.7 (2C), 122.1, 121.0, 116.4, 114.2 (2C), 100.7, 72.1, 65.4, 49.2, 23.1, 17.1, −1.4 (3C); IR (neat, cm^{-1}): 3719 (w, br), 3412 (w, br), 2947 (w, br), 1587 (m), 1466 (w), 1072 (w), 835 (w), 667 (m); HRMS (APCI/ASAP+, *m/z*): found 460.2533 (calcd. $C_{26}H_{34}N_5OSi$, 460.2533 $[M+H]^+$).

4.3.11. (R)-N-(4-(4-((1-Phenylethyl)amino)-7-((2-(trimethylsilyl)ethoxy)methyl)-7H-pyrrolo[2,3-d]pyrimidin-5-yl)phenyl)acrylamide (6k)

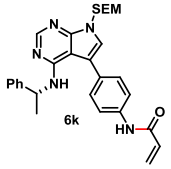

Compound **6j** (176 mg, 0.354 mmol) was dissolved in CH_2Cl_2 (3 mL) and ethyl di-isopropylamine (0.0740 mL, 0.425 mmol) and cooled to 0 °C. Acryloyl chloride (35.0 µL, 0.389 mmol) was added dropwise under a nitrogen atmosphere. The reaction mixture was stirred for 1.5 h, before it was quenched with a saturated $NaHCO_3$ solution (30 mL) and EtOAc (50 mL). The phases were separated and the water phase was extracted with more EtOAc (2 × 30 mL) and the combined organic phases were dried over Na_2SO_4 and concentrated in vacuo. Purification by silica gel column chromatography (EtOAc/*n*-pentane, 3/1, $R_f = 0.54$) gave 183 mg (0.357 mmol, 94%) of a semi-pure yellow oil; ^{1}H NMR (400 MHz, DMSO-d_6): 10.24 (s, 1H), 7.96 (s, 1H), 7.70–7.65 (m, 3H), 7.32–6.93 (m, 7H), 6.51–6.44 (m, 1H), 6.51–6.44 (m, 1H), 6.31–6.26 (m, 1H), 5.78–5.77 (m, 1H), 5.72 (m, 1H), 5.45–5.42 (m, 1H), 5.29–5.23 (m, 1H), 3.64–3.60 (m, 2H), 1.23–1.17 (m, 3H), 0.85–0.81 (m, 2H), −0.12 (s, 9H); HRMS (APCI/ASAP+, *m/z*): found 514.2628 (calcd. $C_{29}H_{36}N_5O_2Si$, 514.2638 $[M+H]^+$).

4.3.12. (S)-2-Phenyl-2-((5-phenyl-7-((2-(trimethylsilyl)ethoxy)methyl)-7H-pyrrolo[2,3-d]pyrimidin-4-yl)amino)ethan-1-ol (7a)

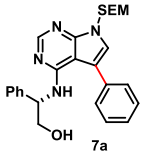

Synthesis of compound **7a** was performed as described in Section 4.3.1 using compound **5** (218 mg, 0.427 mmol) and phenylboronic acid (60 mg, 0.484 mmol). The reaction time was 5 min. Purification by silica-gel column chromatography (CH_2Cl_2/EtOAc, 1/1, $R_f = 0.61$) gave a product contaminated with what appeared to be phenylboronic acid. This was removed by extraction using EtOAc (50 mL) and aqueous NaOH (0.5 M, 30 mL) giving 102 mg (0.222 mmol, 52%) of compound **7a** as a pale yellow oil; $[\alpha]_D^{20} = -12.0$ (c = 1.00, $CHCl_3$); ^{1}H NMR (400 MHz, DMSO-d_6): 8.18 (s, 1H), 7.58–7.56 (m, 2H), 7.53–7.50 (m, 2H), 7.47 (s, 1H), 7.43–7.39 (m, 1H), 7.30–7.25 (m, 4H), 7.23–7.18 (m 1H), 5.99 (d, $J = 7.1$ Hz, 1H), 5.55 (s, 2H), 5.33–5.29 (m, 1H), 4.95 (t, $J = 4.6$ Hz, 1H), 3.76–3.54 (m, 4H), 0.86–0.82 (m, 2H), −0.08 (s, 9H); ^{13}C NMR (100 MHz, DMSO-d_6): 155.6, 151.8, 150.5, 141.4, 134.4, 129.2 (2C), 128.5 (2C), 128.1 (2C), 127.1, 126.7, 126.6 (2C), 123.5, 115.9, 100.3, 72.3, 65.6, 64.6, 55.5, 17.2, −1.36; IR (neat, cm^{-1}): 3413 (w), 3061 (w), 1589 (s), 1467 (m), 1283 (m), 1247 (m), 1182 (m), 1071 (s, br), 758 (s), 640 (m); HRMS (APCI/ASAP, *m/z*): found 461.2368 (calcd. $C_{26}H_{33}N_4O_2Si$, 461.2373, $[M+H]^+$).

4.3.13. (S)-3-(4-((2-Hydroxy-1-phenylethyl)amino)-7-((2-(trimethylsilyl)ethoxy)methyl)-7H-pyrrolo[2,3-d]pyrimidin-5-yl)phenol (7b)

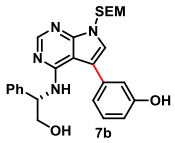

Synthesis of compound **7b** was performed as described in Section 4.3.1 using compound **5** (255 mg, 0.500 mmol) and 3-hydroxyphenylboronic acid (73 mg, 0.529 mmol). The reaction time was 10 min. Purification by silica-gel column chromatography (CH_2Cl_2/EtOAc, 1/1, $R_f = 0.38$) gave 203 mg (0.427 mmol, 85%) as colorless foam, mp = 88–90 °C; $[\alpha]_D^{20} = -112.0$ (c = 1.00, $CHCl_3$); ^{1}H NMR (400 MHz, DMSO-d_6) δ: 9.64 (s, 1H), 8.17 (s, 1H), 7.41 (s, 1H), 7.32–7.28 (m, 5H), 7.23–7.19 (m, 1H), 6.96 (d, $J = 7.7$ Hz, 1H), 6.93–6.92 (m, 1H), 6.82–6.79 (m, 1H), 6.09 (d, $J = 7.4$ Hz, 1H), 5.53 (s, 2H), 5.31–5.28 (m, 1H), 4.92 (t, $J = 4.7$ Hz, 1H), 3.69–3.53 (m, 4H), 0.85–0.81 (m, 2H), −0.08 (s, 9H); ^{13}C NMR (100 MHz, DMSO-d_6) δ: 157.9, 155.6, 151.8, 150.3, 141.3, 135.6, 130.2, 128.2 (2C), 126.8, 126.7 (2C), 123.2, 119.1, 116.1, 115.4, 114.3, 100.3, 72.2, 65.5, 64.7, 55.6, 17.2, −1.36; IR (neat, cm^{-1}): 3401 (w), 3018 (w), 1593 (s), 1470 (m), 1267 (m, br), 1246 (m), 1170 (w), 1069 (s, br), 793 (m), 697 (s) 657 (m); HRMS (APCI/ASAP, *m/z*): found 477.2321 (calcd. $C_{26}H_{33}N_4O_3Si$, 477.2322, $[M+H]^+$).

4.3.14. (S)-2-((5-(4-Methoxyphenyl)-7-((2-(trimethylsilyl)ethoxy)methyl)-7H-pyrrolo[2,3-d]pyrimidin-4-yl)amino)-2-phenylethan-1-ol (7e)

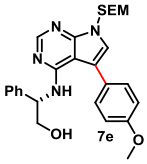

Synthesis of compound **7e** was performed as described in Section 4.3.1 using compound **5** (201 mg, 0.394 mmol) and 4-methoxyphenylboronic acid (77 mg, 0.507 mmol). The reaction time was 10 min. Purification by silica-gel column chromatography (EtOAc/*n*-pentane, 2/1, $R_f = 0.61$). Extraction of the product fractions with 0.5 M NaOH solution, drying over Na_2SO_4 and concentration in vacuo gave 91 mg (0.185 mmol, 47%) of compound **15** as pale red oil; $[\alpha]_D^{20} = -40.0$ (c = 1.00, $CHCl_3$); ^{1}H NMR (400 MHz, DMSO-d_6) δ: 8.16 (s, 1H), 7.48–7.46 (m, 2H), 7.37 (s, 1H), 7.30–7.26 (m, 4H), 7.22–7.20 (m, 1H), 7.07 (d, $J = 8.7$ Hz 2H), 5.98 (d, $J = 7.5$ Hz, 1H), 5.53 (s, 2H), 5.31–5.27 (m, 1H), 4.96 (t, $J = 4.7$ Hz, 1H), 3.81 (s, 3H), 3.74–3.53 (m, 4H), 0.85–0.81 (m, 2H), −0.08 (s, 9H); ^{13}C NMR (100 MHz, DMSO-d_6): 158.5, 155.7, 151.7, 150.3, 141.4, 129.7, 128.1, 126.73, 126.65, 126.5, 122.9, 115.6, 114.6 (2C), 100.5, 72.2, 65.5, 64.6, 55.5, 55.2, 17.4, −1.37; IR (neat, cm^{-1}): 3248 (w), 3030 (w), 2836 (w), 1590 (s), 1467 (m), 1288 (m), 1244 (s), 1175 (m), 1071 (s, br), 697 (m), 658 (m); HRMS (APCI/ASAP, *m/z*): found 491.2479 (calcd. $C_{27}H_{35}N_4O_3Si$, 491.2478, $[M+H]^+$).

*4.3.15. (S)-4-(4-((2-Hydroxy-1-phenylethyl)amino)-7-((2-(trimethylsilyl) ethoxy)methyl)-7H-pyrrolo[2,3-d]pyrimidin-5-yl)phenol (**7i**)*

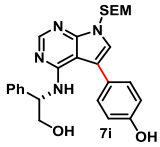

Synthesis of compound **7i** was performed as described in Section 4.3.1 using compound **5** (210 mg, 0.411 mmol) and 4-hydroxyphenylboronic acid (70 mg, 0.508 mmol). The reaction time was 10 min. Purification by silica-gel column chromatography (CH_2Cl_2/EtOAc, 1/1, R_f = 0.46) gave 130 mg (0.273 mmol, 66%) of compound **7i** as a colorless powder, mp. 88–90 °C; $[\alpha]_D^{20}$ = −28.0 (*c* = 1.00, $CHCl_3$); ^{1}H NMR (400 MHz, DMSO-d_6): 9.59 (s, 1H); 8.15 (s, 1H), 7.36–7.34 (m, 2H), 7.31 (s, 1H), 7.29–7.24 (m, 4H), 7.22–7.19 (m, 1H), 6.90 (d, *J* = 9.0 Hz, 2H), 6.00 (d, *J* = 7.0 Hz, 1H), 5.52 (s, 2H), 5.33–5.29 (m, 1H), 4.96 (t, *J* = 5.1 Hz, 1H), 3.73–3.52 (m, 4H), 0.85–0.81 (m, 2H), −0.08 (s, 9H); ^{13}C NMR (100 MHz, DMSO-d_6): 156.7, 155.7, 151.7, 150.2, 141.4, 129.8 (2C), 128.1 (2C), 126.8, 126.6 (2C), 124.8, 122.7, 116.0, 115.9 (2C) 100.6, 72.2, 65.5, 64.6, 55.4, 17.2, −1.35; IR (neat, cm^{-1}): 3395 (w), 3061 (w), 1591 (s), 1470 (m), 1290 (m), 1246 (m), 1177 (m), 1069 (s, br), 697 (s), 642 (m); HRMS (APCI/ASAP, *m/z*): found 477.2322 (calcd. $C_{26}H_{33}N_4O_3Si$, 477.2322, $[M+H]^+$).

*4.3.16. (R)-5-Phenyl-N-(1-phenylethyl)-7H-pyrrolo[2,3-d]pyrimidin-4-amine (**8a**)*

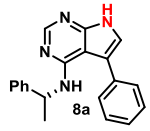

Compound **6a** (169 mg, 0.380 mmol) was dissolved in CH_2Cl_2 (10 mL) and TFA (2 mL). The reaction mixture was stirred at 50 °C for 4.5 h before being cooled and concentrated in vacuo·THF (10 mL) and saturated $NaHCO_3$ (10 mL) were added and the mixture was stirred at 22 °C for 38 h. This only gave 71% conversion to the product. Thus, the concentrated mixture after EtOAc extraction was treated with MeOH (25 mL) and a NH_3-solution (25 mL, 25%) and stirred for 5.5 h. The solvents were removed in vacuo before water (25 mL) and EtOAc (30 mL) were added. After phase separation the water phase was extracted with more EtOAc (2 × 25 mL) and the combined organic phases were dried over Na_2SO_4 and concentrated in vacuo. The product was isolated by silica-gel column chromatography (EtOAc, R_f = 0.26). This gave 109 mg (0.347 mmol, 91%) of **8a** as a white powder; mp. 84–85 °C; HPLC purity: 98%, t_R = 23.1 min; $[\alpha]_D^{20}$ = −124.5 (*c* 1.07, $CHCl_3$). ^{1}H NMR (400 MHz, DMSO-d_6): 11.87 (s, 1H), 8.16 (s, 1H), 7.27 (s, 1H), 7.52–7.45 (m, 4H), 7.39–7.35 (m, 1H), 7.32–7.26 (m, 4H), 7.23–7.19 (m, 1H), 5.44–5.42 (m, 1H), 5.39–5.32 (m, 1H), 1.39 (d, *J* = 6.9 Hz, 3H); ^{13}C NMR (100 MHz, DMSO-d_6): 155.2, 151.5, 150.8, 144.4, 135.1, 128.9 (2C), 128.7 (2C), 128.4 (2C), 126.85, 126.81, 125.8 (2C), 120.3, 115.3, 100.0, 49.4, 22.9; IR (cm^{-1}, neat): 3415 (w), 2980 (w, br), 1580 (s), 1470 (m), 694 (s), 577 (s); HRMS (APCI/ASAP+, *m/z*): found 315.1604, calcd. $C_{20}H_{19}N_4$, 315.1610 $[M+H]^+$)

*4.3.17. (R)-3-(4-((1-Phenylethyl)amino)-7H-pyrrolo[2,3-d]pyrimidin-5-yl)phenol (**8b**)*

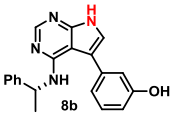

Compound **6b** (100 mg, 0.217 mmol) was dissolved in CH_2Cl_2 (50 mL) and TFA (1 mL, 13.1 mmol). The reaction mixture was stirred at 45 °C for 3 h before the reaction mixture was cooled and concentrated in vacuo·THF (8 mL) and NaOH-solution (2.2 mL, 2 M, 4.26 mmol) were added and the mixture was stirred for 25 h before additional NaOH (0.5 mL, 2 M, 0.40 mmol) was added. Stirring for 3 more hours gave full conversion. Water (20 mL) was added and the aqueous phase was extracted with EtOAc (3 × 20 mL). The combined organic phases were washed with brine (20 mL), dried over anhydrous Na_2SO_4 and concentrated in vacuo. The product was isolated by silica-gel column chromatography (CH_2Cl_2/MeOH, 9/1, R_f = 0.26). Drying gave 60 mg (0.181 mmol, 83%) of **8b** as a beige powder, mp. 130–131 °C; HPLC purity: 96%, t_R = 17.0 min.; $[\alpha]_D^{20}$ = −189.2 (c 1.06, DMSO). ^{1}H NMR (600 MHz, DMSO-d_6): 11.81 (s, 1H), 9.63 (s, 1H), 8.14 (s, 1H), 7.31–7.27 (m, 4H), 7.27–7.25 (m, 1H) 7.22–7.21 (m, 1H), 7.21–7.19 (m, 1H), 6.91–6.90 (m, 1H), 6.89–6.88 (m, 1H), 6.79–6.77 (m, 1H), 5.60–5.59 (m, 1H), 5.36–5.32 (m, 1H), 1.41 (d, *J* = 6.6 Hz, 3H); ^{13}C NMR (150 MHz, DMSO-d_6): 157.8, 155.1, 151.5, 150.7, 144.4, 136.4, 130.0, 128.4 (2C), 126.8, 125.7 (2C), 120.0, 119.3, 115.5 (2C), 113.9, 100.0, 49.3, 23.1; IR (neat, cm^{-1}): 3395 (w, br), 1573 (m), 1476 (m), 1450 (m), 1202 (m),1105 (m), 855 (m), 784 (m), 691 (s); HRMS (APCI/ASAP+, *m/z*): found 331.1553 (calcd. $C_{20}H_{19}N_4O$, 331.1559 $[M+H]^+$).

*4.3.18. (R)-5-(4-Methoxyphenyl)-N-(1-phenylethyl)-7H-pyrrolo[2,3-d] pyrimidin-4-amine (**8e**)*

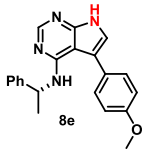

Compound **6e** (49 mg, 0.104 mmol) was dissolved in CH_2Cl_2 (5 mL) and TFA (0.5 mL, 6.55 mmol) and stirred at 50 °C for 2 h. The solvent was removed in vacuo before THF (5 mL) and saturated $NaHCO_3$ (5 mL) were added. The mixture was stirred at room temperature for 19 h and additionally at 40 °C for 28 h. As full conversion was not observed, the reaction mixture was added water (10 mL) and extraction with EtOAc (4 × 10 mL) in order to isolate the product and intermediates. The reaction was then restarted by adding NaOH (42 µL, 5 M, 0.21 mmol) and THF (1 mL) followed by stirring for 18 h at 22 °C. Work-up and purification by silica-gel column chromatography (CH_2Cl_2/MeOH, 9.3/0.7 R_f = 0.40) gave 25 mg (0.080 mmol, 68%) of **8e** as a yellow oil, HPLC purity: 90%, t_R = 21.2 min; $[\alpha]_D^{20}$ = −97.8 (c 0.99, $CHCl_3$); ^{1}H NMR (600 MHz, DMSO-d_6): 11.77 (s, 1H), 8.14 (s, 1H), 7.42–7.40 (m, 2H), 7.31–7.27 (m, 4H), 7.23–7.21 (m, 1H), 7.170–7.166 (m, 1H), 7.04–7.03 (m, 2H), 5.40–5.39 (m, 1H), 5.36–5.31 (m, 1H), 3.80 (s, 3H), 1.40 (d, *J* = 6.9 Hz, 3H); ^{13}C NMR (150 MHz, DMSO-d_6): 158.4, 155.3, 151.4, 150.6, 144.4, 129.9 (2C), 128.4 (2C), 127.3, 126.8, 125.8 (2C), 119.7, 114.9, 114.4 (2C), 100.3, 55.2, 49.4, 22.9; IR (neat, cm^{-1}): 3413 (w), 3101 (w, br), 2919 (w, br), 1584 (s), 1496 (m), 1475 (m), 1252 (m), 1034 (m), 696 (m); HRMS (APCI/ASAP+, *m/z*): found 345.1711 (calcd. $C_{21}H_{21}N_4O$, 345.1715 $[M+H]^+$).

*4.3.19. (R)-N-(4-(4-((1-Phenylethyl)amino)-7H-pyrrolo[2,3-d]pyrimidin-5-yl)phenyl)acrylamide (**8k**)*

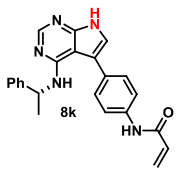

Compound **6k** (122 mg, 0.318 mmol) was mixed with CH_2Cl_2

(10 mL) and TFA (1 mL) and stirred under nitrogen atmosphere at 22 °C for 7 h. The solvent was removed before THF (10 mL) and saturated $NaHCO_3$-solution (10 mL) were added under a nitrogen atmosphere. The mixture was stirred for 18 h, then water (25 mL) and EtOAc (30 mL) were added, the phases were separated and the water phase was extracted with more EtOAc (2 × 25 mL). The combined organic phases were dried over Na_2SO_4 and concentrated in vacuo. The crude product was purified by silica-gel column chromatography (CH_2Cl_2/MeOH, 9/1, R_f = 0.39) to give 23 mg (0.0597 mmol, 25%) of a yellow powder; HPLC purity: 90%, t_R = 19.0 min; $[\alpha]_D^{20}$ = −200 (c 0.97, $CHCl_3$); ^{1}H NMR (400 MHz, DMSO-d_6): 11.83 (s, 1H), 10.26 (s, 1H), 8.14 (s, 1H), 7.79–7.77 (m, 2H), 7.47–7.45 (m, 2H), 7.30–7.28 (m, 4H), 7.24–7.23 (m, 1H), 7.21–7.19 (m, 1H), 6.51–6.44 (m, 1H), 6.31–6.27 (m, 1H), 5.79–5.76 (m, 1H), 5.50–5.48 (m, 1H), 5.40–5.34 (m, 1H), 1.4 (d, J = 6.9 Hz, 3H); ^{13}C NMR (100 MHz, DMSO-d_6): 163.1, 155.2, 151.5, 150.8, 144.5, 137.9, 131.8, 130.2, 129.0 (2C), 128.4 (2C), 127.0, 126.8, 125.8 (2C), 120.1, 119.7 (2C), 115.0, 100.1, 49.4, 23.0; IR (neat, cm^{-1}): 3413 (w), 3096 (w, br), 1579 (s), 1532 (m), 1470 (m), 1408 (m), 1314 (m), 748 (m), 696 (m); HRMS (APCI/ASAP+, m/z): found 384.1819 (calcd. $C_{23}H_{22}N_5O$, 184.1824 $[M+H]^+$).

4.3.20. (R)-5-(3-Aminophenyl)-N-(1-phenylethyl)-7H-pyrrolo[2,3-d]pyrimidin-4-amine (**8m**)

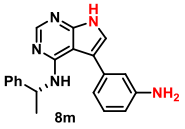

Boc protected **6c** (530 mg, 0.948 mmol) was dissolved in CH_2Cl_2 (50 mL) and TFA (5 mL, 65.5 mmol). The reaction mixture was stirred at 45 °C for 3 h before the reaction mixture was cooled to room temperature and concentrated in vacuo·THF (50 mL) and saturated $NaHCO_3$ (50 mL) were added and the mixture was stirred at 22 °C for 18 h. Following standard work-up, ^{1}H NMR analysis revealed incomplete conversion. Thus, the reaction was restarted using an aqueous NH_3-solution (20 mL, 25%) and MeOH (20 mL). The mixture was stirred over night, before the solvent was removed. Water (50 mL) and EtOAc (50 mL) were added. After phase separation, the aqueous phase was extracted with more EtOAc (2 × 50 mL) and the combined organic phases were dried over anhydrous Na_2SO_4, filtered and concentrated in vacuo. The product was purified twice by silica-gel column chromatography (CH_2Cl_2/MeOH, 9/1, R_f = 0.53). This gave 216 mg (0.657 mmol, 69%) of a beige powder, mp. 93–94 °C (dec.); HPLC purity: 96%, t_R = 19.3 min; $[\alpha]_D^{20}$ = −95.9 (c 1.00, $CHCl_3$). ^{1}H NMR (600 MHz, DMSO-d_6): 11.73 (s, 1H), 8.13 (s, 1H), 7.31–7.27 (m, 4H), 7.22–7.19 (m, 1H), 7.15–7.14 (m, 1H), 7.11 (t, J = 7.8 Hz, 1H), 6.70–6.69 (m, 1H), 6.60–6.59 (m, 1H), 6.58–6.56 (m, 1H), 5.73–5.72 (m, 1H), 5.35–5.31 (m, 1H), 5.26 (br s, 2H), 1.41 (d, J = 6.9 Hz, 3H); ^{13}C NMR (150 MHz, DMSO-d_6): 155.1, 151.4, 150.5, 149.2, 144.5, 135.7, 129.5, 128.4 (2C), 126.7, 125.7 (2C), 119.4, 116.2, 116.0, 113.9, 112.6, 100.1, 49.3, 23.2; IR (neat, cm^{-1}): 3397 (w), 2966 (w), 1569 (s), 1470 (m), 1294 (m), 774 (m), 696 (s); HRMS (APCI/ASAP+, m/z): found 330.1713 (calcd. $C_{20}H_{20}N_5$, 330.1719 $[M+H]^+$).

4.3.21. (S)-2-Phenyl-2-((5-phenyl-7H-pyrrolo[2,3-d]pyrimidin-4-yl)amino)ethan-1-ol (**9a**)

Compound **7a** (154 mg, 0.335 mmol) was dissolved in CH_2Cl_2 (8 mL) and trifluoroacetic acid (2 mL) was added slowly. The mixture was stirred for 2 h at reflux. The solvent was removed by evaporation, and an aq. ammonia (24 mL, 25%) solution and MeOH (12 mL) were added and the mixture stirred at 20 °C for 12 h, before the mixture was concentrated. The residue was mixed with EtOAc (30 mL) and water (25 mL), and after phase separation the water phase was extracted with more EtOAc (3 × 20 mL). The combined organic phase were dried over Na_2SO_4, and concentrated in vacuo. Purification by crystallization from *i*-PrOH using water as anti-solvent, gave 56 mg (0.169 mmol, 51%) of compound **9a** as a colorless powder; mp. 191–192 °C; $[\alpha]_D^{20}$ = −208.0 (c = 1.00, DMSO); ^{1}H NMR (400 MHz, DMSO-d_6): 11.87 (s, 1H), 8.11 (s, 1H), 7.57–7.56 (m, 2H), 7.49 (t, J = 8.3 Hz, 2H), 7.39–7.35 (m, 1H), 7.30–7.25 (m, 5H), 7.22–7.18 (m, 1H), 5.93 (d, J = 7.4 Hz, 1H), 5.34–5.30 (m, 1H), 4.95 (t, J = 5.0 Hz, 1H), 3.74–3.53 (m, 2H); ^{13}C NMR (100 MHz, DMSO-d_6): 155.5, 151.4, 150.9, 141.5, 135.1, 129.0 (2C), 128.5 (2C), 128.1 (2C), 126.69 (2C), 126.68, 126.65, 120.4, 115.5, 100.1, 64.6, 55.4; IR (neat, cm^{-1}): 3418 (w), 3022 (w, br), 1580 (s), 1471 (m), 1114 (m), 1067 (m), 753 (s), 699 (s), 616 (m); HRMS (APCI/ASAP, m/z): found 331.1555 (calcd. $C_{20}H_{19}N_4O$, 331.1559, $[M+H]^+$).

4.3.22. (S)-3-(4-((2-Hydroxy-1-phenylethyl)amino)-7H-pyrrolo[2,3-d]pyrimidin-5-yl)phenol (**9b**)

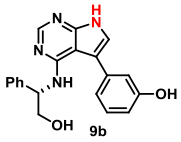

The synthesis was performed as described for **9a** using compound **7b** (185 mg, 0.389 mmol). Purification was performed by silica-gel column chromatography (starting with CH_2Cl_2/MeOH 95/5, then CH_2Cl_2/MeOH 9/1, R_f = 0.03) to give 81 mg (0.234 mmol, 60%) of compound **9b** as colorless powder, mp. 121–122 °C; $[\alpha]_D^{20}$ = −52.0 (c = 1.00, DMSO); ^{1}H NMR (400 MHz, DMSO-d_6): 11.81 (s, 1H), 9.58 (s, 1H), 8.10 (s, 1H), 7–29–7.26 (m, 5H), 7.22–7.19 (m, 2H), 6.96 (d, J = 7.4 Hz, 1H), 6.93–6.92 (m, 1H), 6.79–6.76 (m, 1H), 6.02 (d, J = 7.5 Hz, 1H), 5.33–5.28 (m, 1H), 4.92 (t, J = 5.1 Hz, 1H), 3.72–3.54 (m, 2H); ^{13}C NMR (100 MHz, DMSO-d_6): 157.8, 155.5, 151.4, 150.7, 141.5, 136.4, 130.0, 128.1 (2C), 126.7 (2C), 120.0, 119.2, 115.7, 115.4, 113.8, 100.1, 64.7, 55.5; IR (neat, cm^{-1}): 3114 (w), 1576 (s), 1450 (m), 1066 (m), 785 (m), 698 (m), 646 (m); HRMS (APCI/ASAP, m/z): found 347.1506 (calcd. $C_{20}H_{19}N_4O_2$, 347.1508, $[M+H]^+$).

4.3.23. (S)-2-((5-(4-Methoxyphenyl)-7H-pyrrolo[2,3-d]pyrimidin-4-yl)amino)-2-phenylethan-1-ol (**9e**)

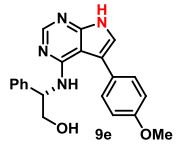

The synthesis was performed as described for **9a** using compound **7e** (89 mg, 0.181 mmol), and reacting with TFA for 6 h. Purification by silica-gel column chromatography (CH_2Cl_2/MeOH, 19/1, R_f = 0.19) gave 34 mg (0.094 mmol, 52%) of **9e** as a colorless crystalline powder, mp. 91–92 °C; $[\alpha]_D^{20}$ = −116.0 (c = 1.00, DMSO); ^{1}H NMR (400 MHz, DMSO-d_6): 11.77 (s, 1H), 8.09 (s, 1H), 7.47 (d, J = 9.0 Hz, 2H), 7.31–7.18 (m, 6H), 7.05 (d, J = 9.0 Hz 2H), 5.91 (d, J = 7.5 Hz, 1H), 5.31–5.27 (m, 1H), 4.95 (t, J = 4.9 Hz, 1H), 3.81 (s, 3H), 3.73–3.54 (m, 2H); ^{13}C NMR (100 MHz, DMSO-d_6): 158.2, 1 55.6, 151.4, 150.6, 141.6, 129.8 (2C), 128.1 (2C), 127.3, 126.7 (2C), 119.8, 115.1, 114.5 (2C), 100.3, 64.6, 55.4, 55.2; IR (neat, cm^{-1}): 3404 (w), 3025 (w), 2833 (w), 1539 (s), 1451 (m), 1175 (m), 1029 (m), 699 (s); HRMS (APCI/ASAP,

m/z): found 361.1661 (calcd. $C_{21}H_{21}N_4O_2$, 361.1665, $[M+H]^+$).

4.3.24. (S)-4-(4-((2-Hydroxy-1-phenylethyl)amino)-7H-pyrrolo[2,3-d] pyrimidin-5-yl)phenol (**9i**)

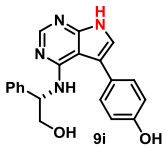

The synthesis was performed as described for **9a** using compound **7i** (105 mg, 0.221 mmol). Purification by crystallization from *i*-PrOH using water as anti-solvent giving 39 mg (0.113 mmol, 51%) of compound **9i** as a colorless powder, mp. 248–249 °C; $[\alpha]_D^{20} = -160.0$ (*c* = 1.00, DMSO); ^{1}H NMR (400 MHz, DMSO-d_6): 11.71 (s, 1H), 9.51 (s, 1H), 8.07 (s, 1H), 7.36–7.33 (m, 2H), 7.31–7.25 (m, 4H), 7.23–7.19 (m, 1H), 7.13 (d, *J* = 2.4 Hz, 1H), 6.87 (d, *J* = 8.5 Hz, 2H), 5.93 (d, *J* = 7.6 Hz, 1H), 5.33–5.28 (m, 1H), 4.95 (t, *J* = 5.4 Hz, 1H), 3.72–3.52 (m, 2H); ^{13}C NMR (100 MHz, DMSO-d_6): 156.4, 155.6, 151.3, 150.5, 141.6, 129.8 (2C), 128.1 (2C), 126.7, 126.6 (2C), 125.5, 119.4, 115.8 (2C), 115.5, 100.3, 64.7, 55.3; IR (neat, cm^{-1}): 3379 (w), 1583 (s, br), 1454 (m), 1106 (m), 1071 (m), 794 (m), 696 (s), 600 (m); HRMS (APCI/ASAP, *m/z*): found 347.1505 (calcd. $C_{20}H_{19}N_4O_2$, 347.1508, $[M+H]^+$).

4.3.25. N-(4-(4-Amino-7H-pyrrolo[2,3-d]pyrimidin-5-yl)phenyl) acrylamide (**10k**)

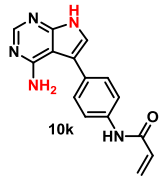

Compound **6k** (172 mg, 0.334 mmol) was dissolved in CH_2Cl_2 (10 mL) and TFA (2 mL) under a nitrogen atmosphere. The reaction mixture was stirred for 3 h at 50 °C before the solvent was removed. The reaction mixture was diluted in MeOH (12 mL) and NH_3 solution (12 mL, 25%) and stirred for 4 h at 22 °C. Water (60 mL) and EtOAc (100 mL) were added to the mixture. The phases were separated and the water phase was extracted with more EtOAc (3 × 40 mL). The combined organic phases were dried over Na_2SO_4 and concentrated in vacuo. The crude product was purified by silica-gel column chromatography (CH_2Cl_2/MeOH, 9/1, R_f = 0.15) to give 30 mg (0.106 mmol, 32%) of a pale yellow powder, mp. 280 °C (dec); HPLC purity: 99%, t_R = 13.0 min; ^{1}H NMR (400 MHz, DMSO-d_6): 11.76 (s, 1H), 10.24 (s, 1H), 8.10 (s, 1H), 7.78–7.76 (ap.d, 2H), 7.43–7.41 (ap.d, 2H), 7.20 (s, 1H), 6.50–6.43 (m, 1H) 6.30–6.25 (m, 1H), 5.99 (s, 2H), 5.79–5.75 (m, 1H); ^{13}C NMR (100 MHz, DMSO-d_6): 163.1, 157.2, 151.7, 151.4, 137.6, 131.9, 130.3, 128.9 (2C), 126.9, 120.1, 119.7 (2C), 115.4, 99.8; IR (cm^{-1}, neat): 3482 (w), 3265 (w), 3098 (w, br), 1654 (s), 1573 (s), 1537 (s), 1537 (m), 965 (w), 898 (w), 794 (s), 731 (m), 607 (m); HRMS (APCI/ASAP+, *m/z*): found 279.1115 (calc. $C_{15}H_{13}N_5O$, $[M]^+$)

4.3.26. 4-Chloro-5-iodo-7-(4-methoxybenzyl)-7H-pyrrolo[2,3-d] pyrimidine (**11**)

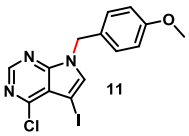

4-Chloro-5-iodo-7*H*-pyrrolo[2,3-*d*]pyrimidine (**2**) (1.01 g, 3.62 mmol) and NaH (0.176 g, 7.34 mmol) were dissolved in dry DMF (5 mL) and cooled to 0 °C. The reaction mixture was stirred for 1 h, before 4-methoxybenzyl chloride (0.60 mL, 4.43 mmol) was added dropwise over 30 min. Then, cooling was removed, and the reaction mixture was stirred until full conversion of the starting materials (3 h). Water (50 mL) and EtOAc (50 mL) were added, the phases were separated. The water phase was extracted with more EtOAc (3 × 50 mL). The combined organic phases were dried over Na_2SO_4, filtered and concentrated in vacuo. Purification of the crude product was done by silica-gel column chromatography (CH_2Cl_2/EtOAc, 10/1, R_f = 0.20) to give 0.940 g (2.35 mmol, 66%) of compound **11** as colorless needle crystals, mp. 136–138 °C; ^{1}H NMR (400 MHz, DMSO-d_6): 8.67 (s, 1H), 8.08 (s, 1H), 7.28 (d, *J* = 8.5 Hz, 2H), 6.88 (d, *J* = 8.5 Hz, 2H), 5.39 (s, 2H), 3.70 (s, 3H); ^{13}C NMR (100 MHz, DMSO-d_6): 158.9, 151.0, 150.6, 150.2, 136.2, 129.3 (2C), 128.7, 116.1, 114.1 (2C), 55.1, 51.8, 47.5; IR (neat, cm^{-1}): 3201 (m), 1514 (s), 1241 (m), 1173 (m), 875 (m), 837 (m), 751 (s), 660 (m); HRMS (APCI/ASAP, *m/z*): found 399.9709 (calcd. $C_{14}H_{12}N_3OClI$, 399.9714, $[M+H]^+$).

4.3.27. (S)-2-((5-Iodo-7-(4-methoxybenzyl)-7H-pyrrolo[2,3-d]pyrimidin-4-yl)amino)-2-phenylethan-1-ol (**12**)

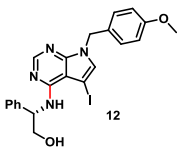

4-Chloro-5-iodo-7-(4-methoxybenzyl)-7*H*-pyrrolo[2,3-*d*]pyrimidine (**11**) (1.02 g, 2.56 mmol) and (*S*)-phenylglycinol (0.990 g, 7.22 mmol) were dissolved in *n*-butanol (10 mL). The reaction mixture was stirred and heated under reflux (145 °C in oil bath temperature) until full conversion was reached (4 h). The solvent was removed in vacuo before EtOAc (90 mL) and water (60 mL) were added. After phase separation, the water phase was extracted with more EtOAc (3 × 90 mL). The combined organic phases were dried over Na_2SO_4 and concentrated in vacuo to give a pale yellow solid. The crude product was purified by recrystallization from *i*-PrOH to give 1.11 g (2.23 mmol, 87%) of compound **12** as a colorless powder, mp. 165–167.5 °C; HPLC purity: 97%, t_R = 23.8; $[\alpha]_D^{20} = -35.0$ (*c* = 1.00, $CHCl_3$); ^{1}H NMR (400 MHz, DMSO-d_6): 8.13 (s, 1H), 7.54 (s, 1H), 7.39 (d, *J* = 7.7 Hz, 2H), 7.34–7.30 (m, 2H), 7.24–7.20 (m, 3H), 7.03 (d, *J* = 7.7 Hz, 1H), 6.86 (d, *J* = 8.6 Hz, 2H), 5.41–5.37 (m, 1H), 5.23–5.20 (m, 3H), 3.86–3.72 (m, 2H), 3.70 (s, 3H); ^{13}C NMR (100 MHz, DMSO-d_6): 158.7, 155.3, 151.9, 149.0, 141.5, 129.7, 129.3, 129.1 (2C), 128.2 (2C), 126.8, 126.7 (2C), 114.0 (2C), 103.1, 64.7, 55.1, 55.0, 49.7, 46.8; IR (neat, cm^{-1}): 3138 (m), 1438 (w), 1176 (m), 1144 (m), 1032 (s), 831 (s), 701 (s), 647 (s); HRMS (APCI/ASAP, *m/z*): found 501.0789 (calcd. $C_{22}H_{22}N_4O_2I$, 501.0787, $[M+H]^+$).

4.3.28. (S)-3-(4-((2-Hydroxy-1-phenylethyl)amino)-7-(4-methoxybenzyl)-7H-pyrrolo[2,3-d]pyrimidin-5-yl)phenol (**13b**)

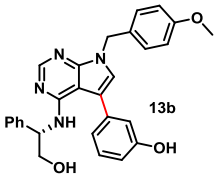

Compound **13b** was made as described in Section 4.3.1 starting with compound **12** (202 mg, 0.404 mmol) and 3-hydroxyphenylboronic acid. The reaction time was 20 h. Purification was done with silica-gel column chromatography (EtOAc, R_f = 0.31) to give 153 mg (0.328 mmol, 81%) as a colorless solid, mp. 94–95 °C; HPLC purity: 99%, t_R = 22.0 min; $[\alpha]_D^{20} = -123.9$ (*c* = 1.00, $CHCl_3$); ^{1}H NMR

(400 MHz, DMSO-d_6): 9.60 (s, 1H), 8.17 (s, 1H), 7.38 (s, 1H), 7.30–7.26 (m, 7H), 7.23–7.19 (m, 1H), 6.94 (d, J = 7.7 Hz, 1H), 6.91–6.90 (m, 1H), 6.87 (d, J = 8.7 Hz, 2H), 6.79–6.76 (m, 1H), 6.08 (d, J = 7.5 Hz, 1H), 5.33–5.30 (m, 3H), 4.93 (t, J = 5.0 Hz, 1H), 3.70–3.53 (m, 5H); ^{13}C NMR (100 MHz, DMSO-d_6): 158.7, 157.9, 155.6, 151.5, 149.5, 141.4, 135.9, 130.2, 130.0, 129.2 (2C), 128.1 (2C), 126.8, 126.7 (2C), 123.0, 119.1, 115.5, 115.3, 114.04, 113.9 (2C), 100.2, 64.7, 55.6, 55.1, 46.6; IR (neat, cm^{-1}): 3077 (m), 2366 (m), 1613 (s), 1155 (m), 1033 (m), 723 (m), 687 (s), 650 (s); HRMS (APCI/ASAP, *m/z*): found 467.2081 (calcd. $C_{28}H_{27}N_4O_3$, 467.2083, $[M+H]^+$).

4.3.29. (5-(4-Amino-7-(2-(dimethylamino)ethyl)-7H-pyrrolo[2,3-d] pyrimidin-5-yl)-2-fluorophenyl)methanol (**15l**)

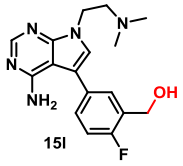

15l

Compound **14** [15] (93 mg, 0.280 mmol), (4-fluoro-3-formylphenyl) boronic acid (55 mg, 0.328 mmol), K_2CO_3 (128 mg, 0.926 mmol), XPhos (4 mg, 0.008 mmol) and XPhos Pd G2 (5 mg, 0.006 mmol) were dissolved in 1,4-dioxane (1 mL) and water (1 mL) under a nitrogen atmosphere. The reaction mixture was stirred at 100 °C for 15 min before water (10 mL) was added and the aqueous phase was extracted with EtOAc (3 × 10 mL). The combined organic phases were washed with brine (10 mL), dried over anhydrous Na_2SO_4, filtered and concentrated in vacuo. The crude aldehyde product was dissolved in THF (10 mL) and MeOH (5 mL) before $NaBH_4$ (34.8 mg, 0.920 mmol) was added. The mixture was stirred for 2 h at room temperature before water (20 mL) was added. The water phase was extracted with EtOAc (3 × 20 mL) and the combined organic phases were washed with brine (20 mL), dried over anhydrous Na_2SO_4, filtered and concentrated in vacuo. Silica-gel column chromatography (CH_2Cl_2/MeOH/NH_3 (25% aq. solution), 80/10/1, R_f = 0.17) gave the product **15l** as a beige powder, 76 mg (0.231 mmol, 81%), mp. 99–100 °C; HPLC purity > 99%, t_R = 6.9 min; ^{1}H NMR (600 MHz, DMSO-d_6): 8.15 (s, 1H), 7.55–7.53 (m, 1H), 7.36–7.33 (m, 2H), 7.26–7.24 (m, 1H), 6.07 (br s, 2H), 5.32 (t, J = 5.6 Hz, 1H), 4.61–4.60 (m, 2H), 4.28 (t, J = 6.5 Hz, 2H), 2.74–2.72 (m, 2H), 2.23 (s, 6H); ^{13}C NMR (150 MHz, DMSO-d_6): 158.6 (d, J = 244.3 Hz), 157.2, 151.5, 150.3, 130.9 (d, J = 3.3 Hz), 129.6 (d, J = 15.3 Hz), 128.8 (d, J = 5.5 Hz), 128.4 (d, J = 7.6 Hz), 123.6, 115.4 (d, J = 22.0 Hz), 114.2, 99.7, 58.2, 56.7 (d, J = 4.4 Hz), 44.9 (2C), 41.3; ^{19}F NMR (376 MHz, DMSO-d_6, C_6F_6): −125.5 (s, dec.); IR (neat, cm^{-1}): 3081 (w, br), 1636 (m), 1595 (s), 1481 (m), 1314 (m), 1205 (m), 1049 (m), 1013 (m), 779 (s), 623 (m); HRMS (APCI/ASAP+, *m/z*): found 330.1728 (calcd. $C_{17}H_{21}N_5OF$, 330.1730 $[M+H]^+$).

4.4. In vitro biochemical assays

4.4.1. In vitro EGFR (ErbB1) inhibitory potency

The compounds were supplied in a 10 mM DMSO solution, and enzymatic EGFR (ErbB1) inhibition potency was determined by Invitrogen (ThermoFisher) using their Z'-LYTE® assay technology [37]. In short, the assay is based on fluorescence resonance energy transfer (FRET). In the primary reaction, the kinase transfers the gamma-phosphate of ATP to a single tyrosine residue in a synthetic FRET-peptide. In the secondary reaction, a site-specific protease recognizes and cleaves non-phosphorylated FRET-peptides. Thus, phosphorylation of FRET-peptides suppresses cleavage by the development reagent. Cleavage disrupts FRET between the donor (i.e., coumarin) and acceptor (i.e., fluorescein) fluorophores on the FRET-peptide, whereas uncleaved, phosphorylated FRET-peptides maintain FRET. A ratiometric method, which calculates the ratio (the emission ratio) of donor emission to acceptor emission after excitation of the donor fluorophore at 400 nm, is used to quantitate inhibition.

All compounds were first tested for their inhibitory activity at 100 nM in duplicates. The potency observed at 100 nM was used to set starting point of the IC_{50} titration curve. The IC_{50} values reported are based on the average of at least 2 titration curves (minimum 20 data points), and were calculated from activity data with a four parameter logistic model using SigmaPlot (Windows Version 12.0 from Systat Software, Inc.) Unless stated otherwise the ATP concentration used was equal to apparent K_M. The inhibitory potency towards $EGFR^{T790M}$ mutant was determined in the same way, but at 500 nM test concentration.

4.4.2. Kinase panel

The compounds were supplied in a 10 mM DMSO solution, and enzymatic kinase inhibition potency was determined by TermoFisher (Invitrogen) using their Z'-LYTE® assay technology [37], at 500 nM in duplicates. ATP concentration used was equal to K_m, except when this service was not provided and other concentrations had to be used.

4.4.3. Ba/F3 cell studies

Transfected Ba/F3 cells containing expression vectors for the $EGFR^{L858R}$ mutant was a kind gift from Dr. Nikolas von Bubnoff at the Technical University of Munich, Munich, Germany [36]. The cells were cultured in RPMI 1640 (Gibco, Invitrogen) supplemented with 10% FCS (Gibco, Invitrogen), 1% L-glutamine (Gibco, Invitrogen) and 0.1% Gentamycin (Sanofi Aventis). Erlotinib was purchased from LC Laboratories (Woburn, MA). All inhibitors were reconstituted in DMSO, and appropriate stock solutions were prepared using cell culture medium. The final percentage concentrations of DMSO were < 0.2%. Proliferation analysis: Ba/F3 cells (1×10^4 per well) were plated into 96-well plates. Inhibitors were added in different concentrations as indicated. Cell growth was measured at 48 h using TACS® XTT Cell Proliferation Assay (Trevigen) according to the manufacturer's instructions. Three independent biological experiments were performed for each compound. All measurements were performed in triplicate.

4.5. Molecular modelling

The X-ray crystal structures of the protein 2J6M (Wild-type EGFR) were prepared using the protein preparation wizard, which is part of the Maestro software package (Maestro, v11.6.013, release 2018–2; Schrödinger, LLC, New York, NY, USA). Bond orders and formal charges were added for het-groups, and hydrogens were added to all atoms in the system. Water molecules beyond 5 Å from het-groups were removed. To alleviate steric clashes that may exist in the original PDB structures, an all-atom constrained minimization was carried out with the Impact Refinement module (Impref) (Impact, v5.0; Schrödinger, LLC) using the OPLS3 force field. The minimization was terminated when the energy converged or the RMSD reached a maximum cutoff of 0.30 Å. The resulting protein structures were used in the following docking study. Ligands were drawn using ChemBioDraw (ChemBioDraw Ultra 13.0, CambridgeSoft, PerkinElmer) and were prepared using LigPrep2.2 (LigPrep, v2.2; Schrödinger, LLC). For the computational investigation of the receptor-inhibitor structures, the energy minimized structures of 2J6M and ligands were subsequently docked using GLIDE in XP mode and Maestro Schrödinger [20–22]. The resulting docked poses were analysed using Glide pose viewer tool. For dynamic simulation, the best poses from docking were used as starting points when building the model systems Dynamic simulations were conducted for 10 ns simulation time using Maestros Desmond suite, the OPLS3e force field and a TIP4P solvent model. Briefly, this was performed by putting the docked protein- ligand complex inside a minimized solvent box and adding ions (Na^+ or Cl^-) in order to have an electrical neutral system. Finally, NaCl was added to a total concentration of 0.15 M, which is approximately the physiological concentration of monovalent ions. This gave normally a system of

approximately 39 000 atoms. Molecular dynamics were then calculated on these systems using the isothermal-isobaric (NPT) ensemble at 300 K and 1.01325 bar. Trajectory analysis were performed using Desmond's Simulation Interactions Diagram tool. All the graphical pictures were made using Maestro.

Acknowledgement

Susana Villa Gonzalez is acknowledged for the HRMS experiments and Roger Aarvik for technical support. Anders Jahres Foundation is thanked for financial support. NOTUR is acknowledged for CPU-time. This work was partly supported by the Research Council of Norway through the Norwegian NMR Platform, NNP (226244/F50).

Appendix A. Supplementary material

Supplementary data to this article can be found online at https://doi.org/10.1016/j.bioorg.2019.102918.

References

[1] W. Pao, J. Chmielecki, Rational, biologically based treatment of EGFR-mutant non-small-cell lung cancer, Nat. Rev. Cancer 10 (2010) 760–774.
[2] Y. Yarden, G. Pines, The ERBB network: at last, cancer therapy meets systems biology, Nat. Rev. Cancer 12 (2012) 553–563.
[3] M.R. Brewer, C.H. Yun, D. Lai, M.A. Lemmon, M.J. Eck, W. Pao, Mechanism for activation of mutated epidermal growth factor receptors in lung cancer, Proc. Natl. Acad. Sci. U. S. A 110 (2013) E3595–E3604.
[4] H.J. Lee, A.N. Seo, E.J. Kim, M.H. Jang, Y.J. Kim, J.H. Kim, S.W. Kim, H.S. Ryu, I.A. Park, S.A. Im, G. Gong, K.H. Jung, H.J. Kim, S.Y. Park, Prognostic and predictive values of EGFR overexpression and EGFR copy number alteration in HER2-positive breast cancer, Br. J. Cancer 112 (2015) 103–111.
[5] J. Koehler, M. Schuler, Afatinib, Erlotinib and Gefitinib in the first-line therapy of EGFR mutation-positive lung adenocarcinoma: a review, Onkologie 36 (2013) 510–518.
[6] A. Sgambato, F. Casaluce, P. Maione, A. Rossi, E. Rossi, A. Napolitano, G. Palazzolo, M.A. Bareschino, C. Schettino, P.C. Sacco, F. Ciadiello, C. Gridelli, The role of EGFR tyrosine kinase inhibitors in the first-line treatment of advanced non small cell lung cancer patients harboring EGFR mutation, Curr. Med. Chem 19 (2012) 3337–3352.
[7] C. Kersten, M.G. Cameron, B. Laird, S. Mjaaland, Epidermal growth factor receptor – inhibition (EGFR-I) in the treatment of neuropathic pain, Br. J. Anaesth. 115 (2015) 761–767.
[8] R.J. Roskoski, ErbB/HER protein-tyrosine kinases: structures and small molecule inhibitors, Pharmacol. Res. 87 (2014) 42–59.
[9] S. Ravez, O. Castillo-Aguilera, P. Depreux, L. Goossens, Quinazoline derivatives as anticancer drugs: a patent review (2011 - present), Expert Opin. Ther. Pat. 25 (2015) 789–804.
[10] S.J. Kaspersen, J. Han, K.G. Nørsett, L. Rydså, E.B. Kjøbli S, G. Bjørkøy, E. Sundby, B.H. Hoff, Identification of new 4-*N*-substituted 6-aryl-7*H*-pyrrolo[2,3-*d*]pyrimidine-4-amines as highly potent EGFR-TK inhibitors with Src-family activity, Eur. J. Pharm. Sci. 59 (2014) 69–82.
[11] J. Han, S. Henriksen, K.G. Nørsett, E. Sundby, B.H. Hoff, Balancing potency, metabolic stability and permeability in pyrrolopyrimidine-based EGFR inhibitors, Eur. J. Med. Chem. 124 (2016) 583–607.
[12] J. Han, S.J. Kaspersen, S. Nervik, K.G. Nørsett, E. Sundby, B.H. Hoff, Chiral 6-aryl-furo[2,3-d]pyrimidin-4-amines as EGFR inhibitors, Eur. J. Med. Chem 119 (2016) 2778–2799.
[13] S. Bugge, A.F. Buene, N. Jurisch-Yaksi, I.U. Moen, E.M. Skjoensfjell, E. Sundby, B.H. Hoff, Extended structure-activity study of thienopyrimidine-based EGFR inhibitors with evaluation of drug-like properties, Eur. J. Med. Chem. 107 (2016) 255–274.
[14] S. Bugge, S.J. Kaspersen, S. Larsen, U. Nonstad, G. Bjørkøy, E. Sundby, B.H. Hoff, Structure-activity study leading to identification of a highly active thienopyrimidine based EGFR inhibitor, Eur. J. Med. Chem. 75 (2014) 354–374.
[15] A.C. Reiersølmoen, J. Han, E. Sundby, B.H. Hoff, Identification of fused pyrimidines as interleukin 17 secretion inhibitors, Eur. J. Med. Chem. 155 (2018) 562–578.
[16] J.D. Becherer, E.E. Boros, T.Y. Carpenter, D.J. Cowan, D.N. Deaton, C.D. Haffner, M.R. Jeune, I.W. Kaldor, J.C. Poole, F. Preugschat, T.R. Rheault, C.A. Schulte, B.G. Shearer, T.W. Shearer, L.M. Shewchuk, T.L. Smalley, E.L. Stewart, J.D. Stuart, J.C. Ulrich, Discovery of 4-amino-8-quinoline carboxamides as novel, submicromolar inhibitors of NAD-hydrolyzing enzyme CD38, J. Med. Chem. 58 (2015) 7021–7056.
[17] A.L. Hopkins, C.R. Groom, A. Alex, Ligand efficiency: a useful metric for lead selection, Drug Discov. Today 9 (2004) 430–431.
[18] C. Abad-Zapatero, J.T. Metz, Ligand efficiency indices as guideposts for drug discovery, Drug Discov. Today 10 (2005) 464–469.
[19] G.M. Keserue, G.M. Makara, The influence of lead discovery strategies on the properties of drug candidates, Nat. Rev. Drug Discov. 8 (2009) 203–212.
[20] Induced fit docking protocol 2013-3, Glide version 6.1, Prime version 3.4, Schrödinger, LLC, New York, NY, 2013.
[21] W. Sherman, H.S. Beard, R. Farid, Use of an induced fit receptor structure in virtual screening, Chem. Biol. Drug Des 67 (2006) 83–84.
[22] W. Sherman, T. Day, M.P. Jacobson, R.A. Friesner, R. Farid, Novel procedure for modeling ligand/receptor induced fit effects, J. Med. Chem. 49 (2006) 534–553.
[23] v. Desmond Molecular Dynamics System, D.E. Shaw Research, Maestro-Desmond Interoperability Tools, version 3.9, Schrödinger, New York, NY, 2014.
[24] C.H. Yun, T.J. Boggon, Y. Li, M.S. Woo, H. Greulich, M. Meyerson, M.J. Eck, Structures of lung cancer-derived EGFR mutants and inhibitor complexes: mechanism of activation and insights into differential inhibitor sensitivity, Cancer Cell 11 (2007) 217–227.
[25] J.H. Park, Y. Liu, M.A. Lemmon, R. Radhakrishnan, Erlotinib binds both inactive and active conformations of the EGFR tyrosine kinase domain, Biochem. J 448 (2012) 417–423.
[26] J. Stamos, M.X. Sliwkowski, C. Eigenbrot, Structure of the epidermal growth factor receptor kinase domain alone and in complex with a 4-anilinoquinazoline inhibitor, J. Biol. Chem 277 (2002) 46265–46272.
[27] H. Park, H.-Y. Jung, S. Mah, S. Hong, Discovery of EGF receptor inhibitors that are selective for the d746–750/T790M/C797S mutant through structure-based de novo design, Angew. Chem., Int. Ed. 56 (2017) 7634–7638.
[28] H. Cheng, S.K. Nair, B.W. Murray, C. Almaden, S. Bailey, S. Baxi, D. Behenna, S. Cho-Schultz, D. Dalvie, D.M. Dinh, M.P. Edwards, J.L. Feng, R.A. Ferre, K.S. Gajiwala, M.D. Hemkens, A. Jackson-Fisher, M. Jalaie, T.O. Johnson, R.S. Kania, S. Kephart, J. Lafontaine, B. Lunney, K.K.C. Liu, Z. Liu, J. Matthews, A. Nagata, S. Niessen, M.A. Ornelas, S.T.M. Orr, M. Pairish, S. Planken, S. Ren, D. Richter, K. Ryan, N. Sach, H. Shen, T. Smeal, J. Solowiej, S. Sutton, K. Tran, E. Tseng, W. Vernier, M. Walls, S. Wang, S.L. Weinrich, S. Xin, H. Xu, M.-J. Yin, M. Zientek, R. Zhou, J.C. Kath, Discovery of 1-{(3R,4R)-3-[({5-Chloro-2-[(1-methyl-1H-pyrazol-4-yl)amino]-7H-pyrrolo[2,3-d]pyrimidin-4-yl}oxy)methyl]-4-methoxypyrrolidin-1-yl}prop-2-en-1-one (PF-06459988), a potent, WT sparing, irreversible inhibitor of T790M-containing EGFR mutants, J. Med. Chem. 59 (2016) 2005–2024.
[29] N. Yamamoto, M. Honma, H. Suzuki, Off-target serine/threonine kinase 10 inhibition by erlotinib enhances lymphocytic activity leading to severe skin disorders, Mol. Pharmacol. 80 (2011) 466–475.
[30] T. Yoshida, K. Yamada, K. Azuma, A. Kawahara, H. Abe, S. Hattori, F. Yamashita, Y. Zaizen, M. Kage, T. Hoshino, Comparison of adverse events and efficacy between gefitinib and erlotinib in patients with non-small-cell lung cancer: a retrospective analysis, Med. Oncol. 30 (2013) 1–7.
[31] M.W. Karaman, S. Herrgard, D.K. Treiber, P. Gallant, C.E. Atteridge, B.T. Campbell, K.W. Chan, P. Ciceri, M.I. Davis, P.T. Edeen, R. Faraoni, M. Floyd, J.P. Hunt, D.J. Lockhart, Z.V. Milanov, M.J. Morrison, G. Pallares, H.K. Patel, S. Pritchard, L.M. Wodicka, P.P. Zarrinkar, A quantitative analysis of kinase inhibitor selectivity, Nat. Biotechnol. 26 (2008) 127–132.
[32] W.L. Tam, H. Lu, J. Buikhuisen, B.S. Soh, E. Lim, F. Reinhardt, Z.J. Wu, J.A. Krall, B. Bierie, W. Guo, X. Chen, X.S. Liu, M. Brown, B. Lim, R.A. Weinberg, Protein kinase C α is a central signaling node and therapeutic target for breast cancer stem cells, Cancer Cell 24 (2013) 347–364.
[33] R.K. Singh, S. Kumar, P.K. Gautam, M.S. Tomar, P.K. Verma, S.P. Singh, S. Kumar, A. Acharya, Protein kinase C-α and the regulation of diverse cell responses, Biomol. Concepts 8 (2017) 143–153.
[34] M.B. Abera, M.G. Kazanietz, Protein kinase Cα mediates erlotinib resistance in lung cancer cells, Mol. Pharmacol. 87 (2015) 832–841.
[35] R. Mancinelli, S. Petrungaro, C.L. Mammola, L. Tomaipitinca, A. Filippini, E. Ziparo, C. Giampietri, G. Carpino, A. Facchiano, Multifaceted roles of GSK-3 in cancer and autophagy-related diseases, Oxid. Med. Cell Longev. 2017 (2017) 4629495.
[36] R.K. Kancha, N. von Bubnoff, C. Peschel, J. Duyster, Functional analysis of epidermal growth factor receptor (EGFR) mutations and potential implications for EGFR targeted therapy, Clin. Cancer Res. 15 (2009) 460–467.
[37] B.A. Pollok, B.D. Hamman, S.M. Rodems, L.R. Makings, Optical probes and assays, WO 2000066766 A1, (2000).